Computer Aided Fatigue Life Prediction for Polymers

David Karl Critz

Submitted to the Department of Mechanical Engineering in partial fulfillment of the requirements for the degrees of

BACHELOR OF SCIENCE
MASTER OF SCIENCE
in
MECHANICAL ENGINEERING
at the
MASSACHUSETTS INSTITUTE OF TECHNOLOGY
JUNE 1997

Author.....
Department of Mechanical Engineering
May 9, 1997

Certified by.....
Professor David Wallace
Department of Mechanical Engineering
Thesis Supervisor

Accepted By.....
Ain Sonin
Chairman Graduate Committee

Computer Aided Fatigue Life Prediction for Polymers

David Karl Critz

Submitted to the Department of Mechanical Engineering on May 9, 1997 in partial fulfillment of the requirements for the degrees of Bachelor of Science and Master of Science in Mechanical Engineering.

ABSTRACT

This thesis adapts conventional metals fatigue life prediction methods to allow their use with a polycarbonate plastic. The original program, proprietary Ford Motor Co. software, accepted a service load history, applied it to a finite element mesh of a part to produce a strain history, converted linear strains to nonlinear strains with Neuber's rule, referenced cycle life from a strain-life curve, and summed damage with a Miner rule. The modification which allowed use with polymers was the transformation of the internal strain-life relation from a 4-parameter fit to a digitized nonparametric curve.

Physical testing was directed toward generating data files for program input, evaluating total prediction performance, and evaluating the performance of individual program components. The program was found to predict within a factor of two of the actual time to fracture initiation during bench tests with a typical plastic automotive component. Most of the error in the prediction can be attributed to the polycarbonate's tendency to survive varying numbers of cycles to initiation under identical load histories and part geometries. This strain-life scatter is the result of material sensitivity to small changes in test conditions and variations in the plastic itself. The Neuber correction component was tested using notched samples, but the mostly elastic test range caused results to be inconclusive. The Miner rule component of the program was tested and found to be a small contributor to prediction error.

The second largest contributor to prediction error was evaluation of the part's strain history. This is the most promising area for improvement to the method.

Thesis Supervisor: David Wallace
Title: Esther and Harold E. Edgerton Assistant Professor

Table of Contents

List of Figures

List of Tables

List of Nomenclature

$\Delta\varepsilon_a$	total strain amplitude
$\Delta\varepsilon_p$	elastic strain amplitude
$\Delta\varepsilon_p$	plastic strain amplitude
σ_m	mean stress
σ_{max}	maximum stress.
$\Delta\sigma$	stress amplitude
σ'_f	Fatigue strength coefficient
b	Fatigue strength exponent
E	Young's modulus of elasticity
ε'_f	Fatigue ductility coefficient
c	Fatigue ductility exponent
$2N_i$	Number of cycles to initiation
$2N_f$	number of cycles to total failure
K'	cyclic strength coefficient
n'	cyclic strain hardening exponent.
σ	elastic-plastic cyclic stress (actual)
ε	elastic-plastic cyclic stress (actual)
S	linear elastic FEA stress (nominal)
e	linear elastic FEA strain (nominal)
D	cumulative damage (0.0 = undamaged, 1.0 = crack initiation)
$2N_{(i)}$	Number of cycles at strain amplitude "i"
$(2N_i)_{(i)}$	Number of cycles to initiation at strain amplitude "i"

Acknowledgments

This thesis was conducted through the Massachusetts Institute of Technology Engineering Internship Program in cooperation with the Ford Motor Company in Dearborn, MI. The author would like to thank Ford for participating in EIP. The author is indebted to the following people for their advice and support:

- Dave Wallace, MIT Department of Mechanical Engineering
- Peter Stahle, MIT Department of Nuclear Engineering
- Al Conle, Ford SRL
- Lokesh Juneja, Ford AVT
- Ravi Thyagarajnan, Ford ACD
- Jim Lengyel, Ford Central Lab

In recognition for boundless tolerance regarding time spent in lab: Rebecca Harley

For support both moral and financial: Mark & Susan Critz

1. INTRODUCTION

Engineering analysis with polymer materials is currently constrained by the difficulty of predicting long-term life in cyclic loading. Empirical relations used in metals to predict fracture initiation are complicated by environmental and viscoelastic factors to which polymers are especially sensitive. The frequent introduction of new materials makes it impractical to test every engineering plastic for its fatigue properties. The polymer fatigue data which exists is often proprietary or inconsistently tested. As a result, a complete polymer fatigue database and a method with which to transform data into predictions are not available.

Three trends combine to make the development of this predictive capability imperative:

1. Increasing polymer content in new products such as automobiles. This pushes plastics from decorative to structural applications and increases applied loads.

2. Reduced new product development budgets and time cycles. Physical testing of components is expensive, time-intensive, and limits iteration.

3. Increasing customer requirements for product durability. All parts will be expected to endure extended use.

Plastics design lacks the durability methodologies and extensive material databases (Takemori 1981) which are already mature for metals (Mitchell 1987). The goal of this thesis was to determine the applicability of existing methods to polymer materials given sufficient information about a common polycarbonate material. This was accomplished through gathering material properties for GE Lexan EM3110 automotive interior grade polycarbonate and evaluating the applicability of classical fracture behavior rules, then applying the data and methods to a test case.

This section provides an overview of the durability analysis process and gives background information on polymers in cyclic loading. The second section covers the four types of physical tests conducted for this thesis: (1) strain-life curve generation, (2) Neuber's rule evaluation, (3) Palmgren-Miner rule verification, and (4) a component bench test. It will be followed with a discussion of potential future research direction and a few concluding thoughts.

1.1 Computer-Aided Durability Analysis

Durability analysis was originally applied to metal components under constant sinusoidal loads. As data collecting and analytical tools have improved, load patterns and analyzed geometries have become increasingly complex. Modern ground vehicle durability analysis involves characterizing three basic relationships (Fash 1987):

1. Environment-Load: This involves obtaining road-load data by instrumenting a prototype vehicle with load cells or accelerometers at key locations. This vehicle is then driven on test track surfaces which represent a best guess of end use conditions (Devlukia 1987). It is also possible to predict road inputs computationally without the use of a test track and prototype (Thomas 1987). As end-use of any product is unpredictable and variable, this step requires significant approximation.

2. Load-Strain: This step uses finite element analysis to transform load inputs into a stress or strain history (Heyes 1995). The analysis can be static or dynamic, linear or nonlinear. Each strain amplitude experienced by the part is recorded for later use (Hay 1987). As FEA procedures always involve some degree of error, this step introduces another level of approximation.

3. Strain-Life: This step treats a strain-life curve as a material property and applies that curve to each strain amplitude experienced by an element of the FE mesh, then uses some damage accumulation rule to account for varying strain amplitudes. The strain-life curve used is typically generated without regard to multiaxiality, environmental conditions, aging, frequency, waveform, or other factors. This introduces yet another level of approximation.

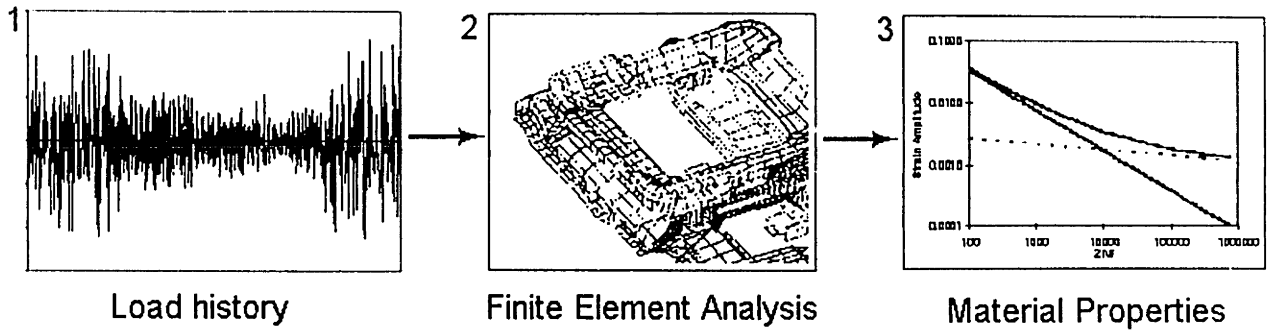

Figure 1-1: The Durability Analysis Process

Once these three relationships are known, it is possible to generate an estimate for the mechanical fatigue life of a part. Iteration, either through varying material, geometry, or load inputs, can then serve to optimize the design. These steps as they are applied to a functioning durability analysis program will be described in section 1.3.

1.2 The Importance of Material Properties

Effort must be concentrated upon the third relationship in order to apply this methodology to plastic materials. Environment-load data collection and finite element analysis (the first two relationships) have been used on plastic components for years and do not require much additional development. By comparison, fatigue behavior of polymers a significant unknown. Existing materials databases are insufficient and often proprietary. Even with a useful database, it is still unknown whether the existing methodology can be used with polymers (Takemori and Morelli 1981). Further investigation of polymer fatigue properties can gain valuable lessons from what is already known about metals.

Research into fatigue properties of metals is broken down into two broad categories: propagation and initiation. Both are mature fields with large public-domain databases listing material properties (Rice et al 1988, ASM 1986). Propagation data is necessary for the defect-tolerant design most often used in the aerospace industry. Since an uncracked part can take much more time to initiate a crack than propagate one, defect-tolerant methods result in design and inspection requirements which are conservative for ground vehicle applications. Most durability analysis programs assume an initially unflawed component and calculate the number of cycles until crack initiation.

As there is no mechanistic model which will allow the prediction of this relationship, most programs will use a strain-life curve determined from physical experiments.

1.3 The Fatigue Life Analysis Procedure (FLAP) Program

This investigation will build upon FLAP, an existing proprietary metals analysis program (Agrawal, Conle, et al 1996), modifying critical sections for use with plastics. Background material for program concepts will be discussed in section 2.1.

In order to use FLAP, the user must have three files:

1) A finite element analysis with a unit-load subcase defined for each loading point

2) A load history for each loading point

3) A material property listing which defines the four Coffin-Manson strain-life parameters and the three Ramberg-Osgood cyclic stress-strain numbers

FLAP processes these three input files through the following eight steps to produce a fatigue life prediction:

The FLAP Process

1) From a static analysis, generate an influence factor which gives the stress in each element as a result of a unit load applied to each load point.

2) Create a histogram for the principal stresses and their critical plane angles given the load sequence for each load point to determine a unique principal plane angle.

3) Calculate uniaxial Von Mises stresses perpendicular to the principal plane for each element and time index.

4) Simplify the stress-time history by performing a rainflow count. (See section 2.1.6 for details)

5) Convert the linear-elastic stress rainflow count into an elastic-plastic strain rainflow history using Neuber's rule. (See section 2.1.3 for details) Record upper and lower bound mean stresses.

6) Calculate damage using each element's mean stress and strain amplitude history. Use Coffin-Manson simple strain, Morrow's Stress correction, and the Smith-Watson-Topper stress correction. (See section 2.1.1 for details)

7) Sum damage from each strain amplitude and stress level using the Palmgren-Miner rule (See section 2.1.5 for details).

8) Transform cumulative damage to a fatigue life estimate.

Each step introduces an additional level of approximation, causing errors to propagate and accumulate through the procedure. Controlled laboratory experiments (SAE 1989) on metal test bars using this methodology can generate predictions within a factor of two of the experimental result.

In order to modify this program for use with plastic materials, step 6 will be modified to accept strain-life curves which do not fit Coffin-Manson parameters. The assumptions underpinning steps 5 and 7 will be evaluated with physical testing.

2. BACKGROUND INFORMATION

This paper concerns itself with the intersection of two fields - fracture mechanics and polymers. Background in the former is provided here. Polymers in cyclic loading will be discussed later in section 2.

2.1 Durability Analysis Concepts

This section provides information needed to understand the theory behind the FLAP program.

2.1.1 The Strain-Life Curve

For metals the strain-life curve is the sum of two components, the plastic ($\Delta\varepsilon_p$) and elastic ($\Delta\varepsilon_e$) strain amplitudes. The magnitudes of these components (the sum of which is the total imposed strain $\Delta\varepsilon_a$) can be determined from examining the hysteresis curve formed while cycling at a constant strain. (See Figure 2-2) Both strains usually vary log-log linearly with cycles to failure, allowing the total strain-life curve to be fit to the vertical sum of each line. The relationship typically resembles Figure 2-1:

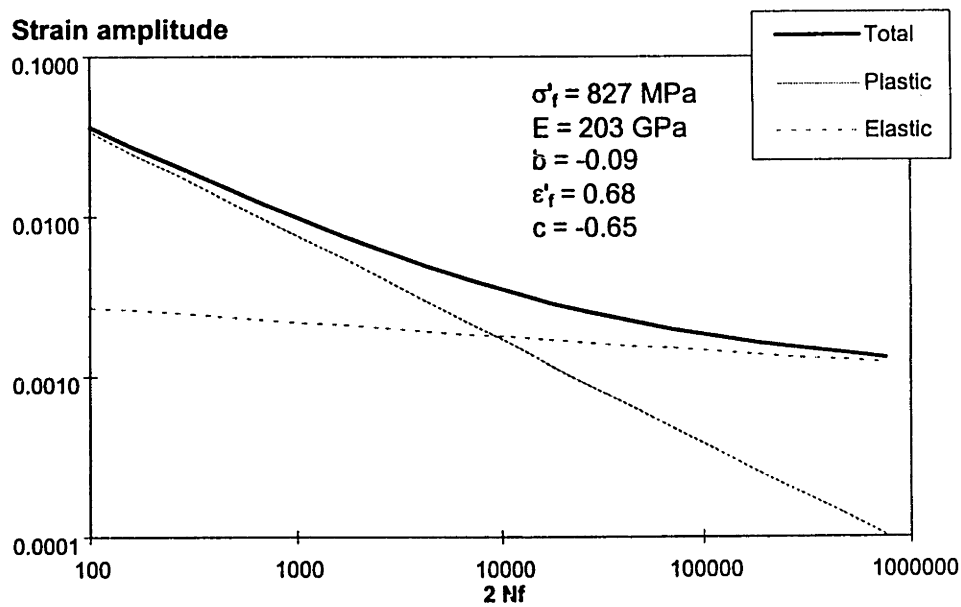

Figure 2-1: Strain-Life for SAE 950X

This behavior is described by the Coffin-Manson empirical fit:

$$(2.1) \qquad \Delta\varepsilon_a = \Delta\varepsilon_e + \Delta\varepsilon_p = \frac{\sigma'_f}{E}(2N_i)^b + \varepsilon'_f(2N_i)^c$$

where $\Delta\varepsilon_a$ = total strain amplitude
$\Delta\varepsilon_p$ = elastic strain amplitude
$\Delta\varepsilon_p$ = plastic strain amplitude
σ'_f = Fatigue strength coefficient
b = Fatigue strength exponent
E = Young's modulus of elasticity
ε'_f = Fatigue ductility coefficient
c = Fatigue ductility exponent
$2N_i$ = Number of cycles to initiation

The four numbers σ'_f, ε'_f, b, and c are the Coffin-Manson fit parameters.

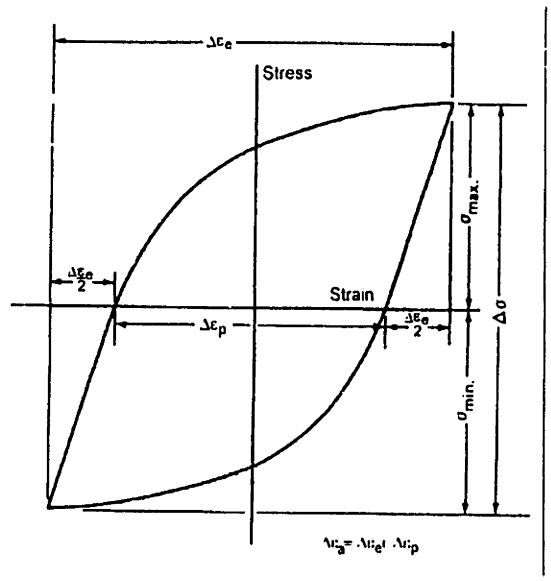

Figure 2-2: Decomposing $\Delta\varepsilon_p$ and $\Delta\varepsilon_e$ (Conway & Sjodahl 1991)

Other researchers have suggested improvements upon the Coffin-Manson fit which take into account additional loading factors. The two used by FLAP are Morrow's mean stress correction (Dowling 1993):

$$(2.2) \qquad \Delta\varepsilon_a = \frac{\sigma'_f - \sigma_m}{E}(2N_f)^b + \varepsilon'_f(2N_f)^c$$

where σ_m = mean stress

and the Smith-Watson-Topper stress correction (Dowling 1993):

$$(2.3) \qquad \sigma_{max}\Delta\varepsilon_a = \frac{(\sigma'_f)^2}{E}(2N_f)^{2b} + \sigma'_f\varepsilon'_f(2N_f)^{b+c}$$

where σ_{max} = maximum stress.

Extensive research has been invested in determining the strain-life effects of mean stress, waveform, strain rate, environment, temperature, annealing, and impurities (Conway & Sjodahl 1991).

2.1.2 Cyclic Stress-Strain Behavior

Cycling will alter the stress-strain properties of a metal - it can either harden or soften during cyclic loading. In metals, the same state will be reached in both stress and strain control: if a specimen is cycled at constant strain X and stabilizes at stress Y, it will also stabilize at strain X if cycled at constant stress Y (Conway & Sjodahl, 1991). If one plots the stable cyclic stress level against each tested strain level and connects the tips of the hysteresis loops, it is possible to generate a cyclic stress-strain curve which is very different from the standard monotonic curve.

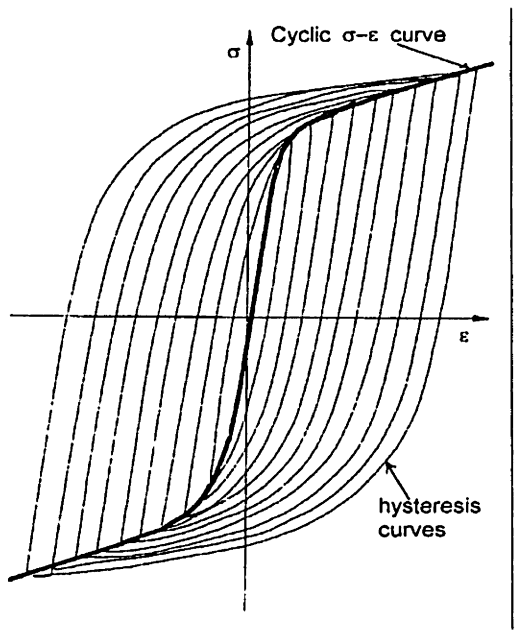

Figure 2-3: Generating a cyclic stress-strain curve (SAE J1099, 1977)

The Ramberg-Osgood fit describes the cyclic stress-strain curve by breaking the stress components into elastic and plastic components (Dowling 1993). The plastic component (Equation (2.5)) is assumed to be log-log linear, an assumption which can break down at very low strains.

(2.4) Elastic: $\sigma_a = E\varepsilon_e$

(2.5) Plastic: $\sigma_a = K'\varepsilon_p^{n'}$

(2.6) Combined: $\varepsilon_a = \varepsilon_e + \varepsilon_p = \frac{\sigma_a}{E} + \left(\frac{\sigma_a}{K'}\right)^{\frac{1}{n'}}$

where σ_a = applied stress

ε_p = plastic strain
K' = cyclic strength coefficient
n' = cyclic strain hardening exponent.

Note that this fit assumes equal stress-strain behavior in both tension and compression. Care must be taken to correct for necking during stress calculations or the data will not be log-log linear at high plastic strain amplitude.

Ideally, the factors K' and n' are not independent of the Coffin-Manson parameters. From equation (2.1) elastic strain is defined as $\varepsilon_e = \frac{\sigma_a}{E} = \frac{\sigma_f'\left(2N_f\right)^b}{E}$, so solving for the stress amplitude gives $\sigma_a = \sigma_f'\left(2N_f\right)^b$. Also from equation (2.1), the plastic strain is $\varepsilon_p = \varepsilon_f'\left(2N_f\right)^c$. Eliminating $2N_f$ between both expressions gives

$$(2.7) \qquad \sigma_a = \frac{\sigma_f'}{\left(\varepsilon_f'\right)^{\frac{b}{c}}}\varepsilon_p^{\frac{b}{c}}$$

, a σ-ε_p relationship derived entirely from the Coffin-Manson relationship. If this is compared with equation (2.5), it is seen that

$$(2.8)\ n' = \frac{b}{c}$$

$$(2.9)\ K' = \frac{\sigma_f'}{(\varepsilon_f')^{n'}}.$$

In reality, independent fits of the six parameters rarely meet this relationship exactly. Most metals display behavior close to the relationship, but some materials may display a large inconsistency between independently fit K' and n' values and the values derived from the Coffin-Manson parameters. This is usually due to a deviation of the data points from the log-log linear fit lines. Provided that the strain-life and stress-strain curves fit the data well, an analysis based upon independently-fit numbers will not be negatively affected by the failure to meet the relationship between the six parameters (Dowling 1993).

2.1.3 Neuber's Rule

Since finite element analysis is generally linear-elastic, some attempt must be made to transform FEA results to fit the elastic-plastic nature of the cyclic stress-strain curve. Neuber's rule (Tipton 1991) provides a bridge between the two forms. The finite element program output is generally linear elastic nominal stress. This leaves three unknowns which demand three equations in order to solve for the elastic-plastic stress and strain. The first equation is Neuber's Rule. The second and third describe the linear elastic and elastic-plastic stress-strain curves:

(2.10) Neuber's Rule: $\sigma\varepsilon = Se$

(2.11) Linear-Elastic: $e=S/E$

(2.12) Elastic-Plastic: $$\varepsilon_a = \frac{\sigma_a}{E_a} + \left(\frac{\sigma_a}{K'}\right)^{\frac{1}{n'}}$$

where: σ = elastic-plastic cyclic stress (actual)
ε = elastic-plastic cyclic stress (actual)
S = linear elastic FEA stress (nominal)
e = linear elastic FEA strain (nominal)

Graphically, the solution of this equation can be represented by Figure 2-4. For any given linear-elastic stress-strain product, there is a unique corresponding equal elastic-plastic stress-strain product. The stress-strain product of the linear-elastic solution (S*e) is the area of the colored box. The stress-strain product of the elastic-plastic solution (σ*ε) is represented by the area of the hashed-colored box. The areas of these two boxes must be equal.

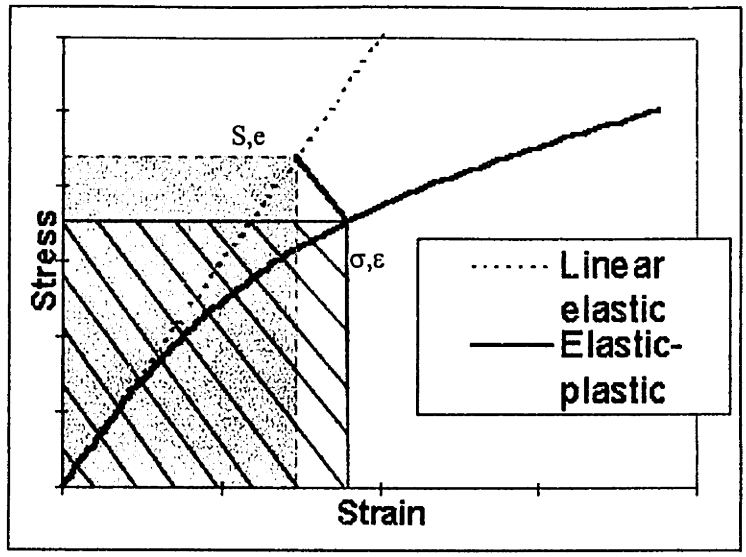

Figure 2-4: Neuber's Rule

Neuber's rule was originally developed for use in prismatic bodies experiencing pure shear. It makes its most accurate predictions at low (mostly elastic) stresses in thin sheets (Tipton 1991). Neuber's rule generally gives acceptable results and is widely used due to its conservatism: if it errs, it tends to overpredict strain amplitudes (Leis Gowda & Topper 1973, Seeger & Heuler 1980). Modifications to Neuber's rule have been proposed which add notch sensitivity parameters (Buch 1975) or equate the strain energy (area under each stress-strain curve) instead of the stress-strain product (Glinka 1985). Despite the increased accuracy of these methods, the extra testing, increased computational demands, or nonconservativism of these modified methods has caused the standard Neuber's rule to remain a widely accepted tool.

2.1.4 Unloading Behavior

Complicated random loading histories can cause any given cycle to originate from almost any point in stress-strain space. As such it is necessary to have an equation which describes the unloading curve, the shape of one reversal on the hysteresis loop. If the cyclic stress-strain curve is already characterized with the Ramberg-Osgood equation, equation (2.13) will describe the unloading curve (Dowling 1993):

$$(2.13)\quad \frac{\varepsilon_a}{2} = \frac{\sigma_a / 2}{E_a} + \left(\frac{\sigma_a / 2}{K'}\right)^{\frac{1}{n'}}$$

The only difference between this equation and the Ramberg-Osgood relation is the factor of two applied to the stress and strain quantities. This factor essentially magnifies the cyclic stress-strain curve by a factor of 2 in both the X and Y directions. When cycling between two points on the cyclic stress-strain curve, the unloading curve must touch the endpoints of the magnified average cyclic σ–ε curve. Figure 2-5 shows the unloading curve of the steel from Figure 2-3 compared to magnified plots of the compressive, tensile, and average cyclic stress-strain curves.

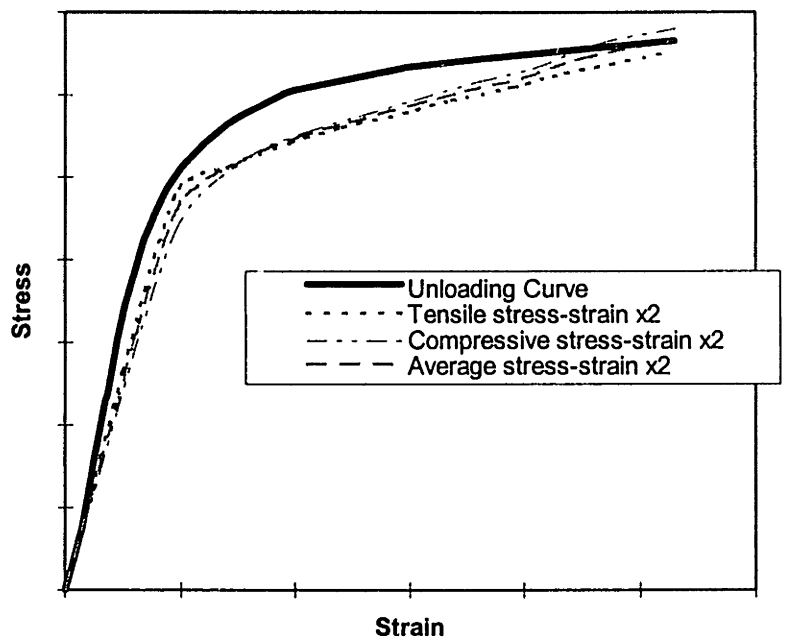

Figure 2-5: Factor-of-two approximation of the unloading curve

Note that the scaled average of the tensile and compressive cyclic stress-strain curves does indeed touch the unloading curve at its beginning and end points. This graph was generated from the largest hysteresis loop in Figure 2-3.

The unloading curve will give the same strain amplitude regardless of the starting point in stress-strain space. This allows efficient simple-strain analysis since it is not necessary to locate the reversal in stress-strain space. Morrow's mean stress correction and the Smith-Watson-Topper correction require knowledge of the strain amplitude as well as the stress at the beginning and end of the reversal. If the full stress history is known, it is possible to use "push-down list" cycle counting (Conle et al 1988) to define the strain amplitude and mean stress history for the part. If sequence effects are not available (as in a history reconstructed from a rainflow count, a procedure described in section 2.1.6), mean stresses can be approximated. This can be accomplished by generating the largest possible

hysteresis loop and then locating each reversal within the area of that loop. Since the maximum and minimum elastic strain are known for all reversals, it is possible to place a lower and upper bound on each reversal's mean stress. Analysis can then be based upon the worst-case result (Agrawal, Conle et al 1996). Since the polymer fatigue life analysis procedure developed later does not consider mean stress effects, further detail on this topic will not be presented.

2.1.5 Damage Accumulation

The Palmgren-Miner rule sums damage sustained at several different strain amplitudes. Assuming a linear accumulation of damage at each strain level, this can be represented mathematically as (Dowling 1993):

$$(2.14) \quad D = \sum \frac{2N_i}{(2N_f)_i}$$

where D = cumulative damage (0.0 = undamaged, 1.0 = crack initiation)
$2N_i$ = Number of cycles at strain amplitude "i"
$(2N_f)_i$ = Number of cycles to failure at strain amplitude "i"

For a pre-defined repeating block of several different strain amplitudes, equation (2.14) gives the damage which results from a single "pass" of this block. The number of passes until failure would then be L = 1/D.

There is little support for the idea that damage accumulates linearly with number of cycles. The evidence to date shows that less damage is sustained during the early portion cycling and most damage occurs as the part nears its fatigue life (Lutes et al 1984). This can be approximated by an altered P-M form with an exponent "m" to describe this nonlinearity. For a constant-strain loading cycle $D = \left(\frac{2N_f}{(2N_f)_i} \right)^m$ A plot of D vs. $2N_i/(2N_f)_i$ for a constant strain amplitude and different values of "m" is shown in Figure 2-6. Palmgren-Miner linear damage accumulation uses m=1, whereas a value of m=3 or 4 has been shown to work best for most metals (Lutes et al 1984).

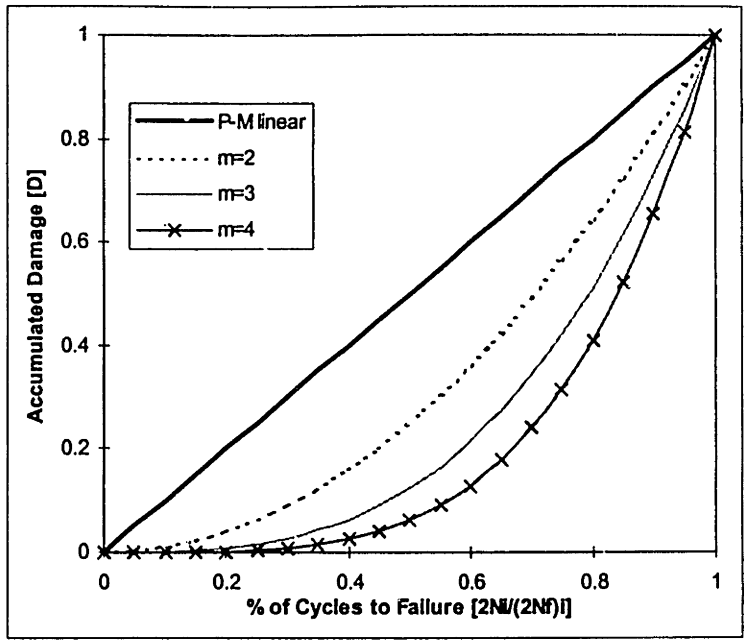

Figure 2-6: Nonlinear Damage Accumulation

Both the strength and weakness of the linear P-M equation is that it is independent of loading order: a low-strain block followed by a high-strain block will have the same predicted life as a high-strain block followed by a low-strain block. This is an advantage since a standard rainflow matrix of strain amplitudes (commonly used in the place of a strain history) does not preserve loading order information. Research has shown, however, that loading order *is* a factor (Miller and Zachariah 1977). If very high strain cycling produces crazing or other micromechanical defects, failure could be accelerated in subsequent low strain cycling, thus producing a much earlier failure than if the load levels had been applied in the opposite order. In a two-step procedure which transitions from low to high strain ranges, Palmgren-Miner will underpredict fatigue life. If the sequence moves from high to low, Palmgren-Miner will overpredict life. Generally, the greater the difference between the two strain levels, the greater the error will be (Miller & Zachariah 1977).

Several modifications to the Palmgren-Miner rule have been proposed which have been shown to give better cumulative damage life predictions (Pompetzki et al 1990, Lutes et all 1984, Iida 1993, Miller & Zachariah 1977, Hashin & Laird 1980, Thang 1971, Manson et al 1967). Unfortunately, these rules are more computationally intensive and require difficult-to-obtain empirical correction factors, load order data, or cycling frequency information. Despite its recognized weaknesses, the Palmgren-Miner linear damage accumulation rule is still

widely used and acknowledged to be an acceptable equation for summing damage from application of varying loads. (Miller & Zachariah 1977).

2.1.6 Rainflow Cycle Counting

In real life, load conditions rarely come in the form of well-defined, repeated blocks of constant strain levels. One must use some cycle counting algorithm to decompose the random form of service inputs into a collection of repeated strain amplitudes. One commonly used method is "rainflow counting" which also has the advantage of storing large amounts of information in a compact form (Dowling 1993). By dividing a time-series plot into discrete "bins" it is possible to define a matrix which describes how many jumps were made from one bin to another. If each bin represents a stress level, each entry in the matrix will describe a different stress amplitude and mean stress level.

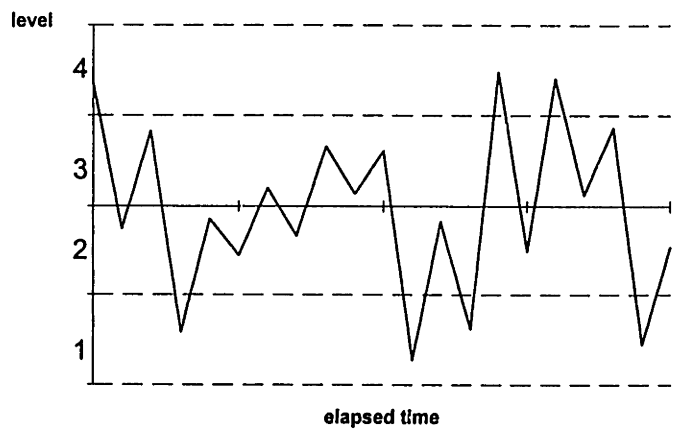

	1	2	3	4
1		3		1
2	1		3	1
3	3	2		
4		2	1	

Figure 2-7: Rainflow Cycle Counting

The numbers in the left column show a reversal's starting bin and the numbers in the top row show a reversal's ending bin. All matrix entries on the lower left of the diagonal line indicate a rising line (trough-to-peak) and all entries in the upper left indicate a falling level (peak-to-trough).

2.2 Fatigue of Polymers

Durability information for plastics is incomplete in comparison to the material database available for metals. The metals industry is introduces new materials infrequently whereas new polymers, new mixes of old polymers, and new additives make the introduction of new materials in the plastics industry almost continuous. Differences in processing conditions and batch properties will introduce significant variation in fatigue properties between parts made of the same material. Testing every possible material and variant would be impractical, if not impossible. Due to the expense and time required by fatigue property testing and the historically nonstructural applications of plastic parts, little need was seen in the past for an extensive database.

2.2.1 Stress vs. Strain Control

What data does exist is typically represented in the form of an S-N curve. This relates a constant applied stress to the log of total cycles to failure. The S-N curve is purely an empirical observation with no supporting mechanistic model. Due to test apparatus limitations, the S-N curve is usually loaded with maximum and minimum applied stress in the tensile range. A tensile-tensile S-N curve has many shortcomings:

1. Stress control can lead to the addition of unwanted viscoelastic factors, such as creep and hysteretic heating (Suresh, 1991).

2. Very few parts are loaded solely in tension, making a tension-tension test an unrealistic representation of the end loading case.

3. Most durability analysis programs relate strain amplitude to life. Using S-N data would require rewriting the program code or using the stress-strain behavior of the material to generate strain-life curves.

These factors combine to make strain control the "most meaningful parameter under which to control fatigue tests" (Beardmore & Rabinowitz 1975).

2.2.2 Polymer Strain-Life Relationships

While metals generally conform to the log-log linear form of the elastic and plastic strain amplitudes used by the Coffin-Manson equation, plastics rarely do. The strain-life plots in Figure 2-8 show cycles to initiation for a variety of polymers.

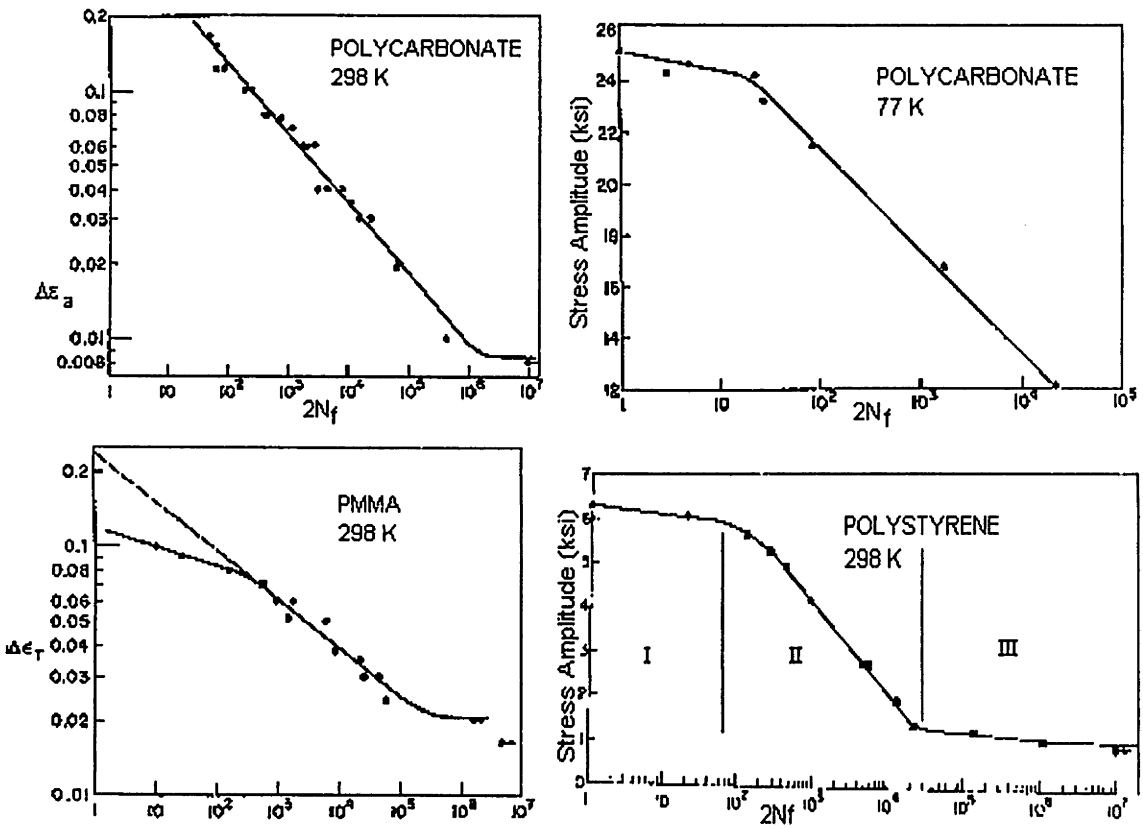

Figure 2-8: Example Strain-Life Curves (Beardmore & Rabinowitz 1975)

The strain-life relationship of polymers follows a general pattern shown in Figure 2-9. Most polymers display log-log linear behavior (region II) and an "endurance limit" (region III) beyond which all life is essentially infinite. In brittle polymers which craze, region I will show a second kink point and a line with a shallower slope than region II behavior indicating a greater sensitivity to applied strain. Common materials displaying craze formation at room temperature include polystyrene, polysulfone, polymethylmethacrylate (PMMA), polyethylene, polypropeline, and polyethyleneteraphthalate (PETP) (Kramer 1983, Kramer & Berger 1990).

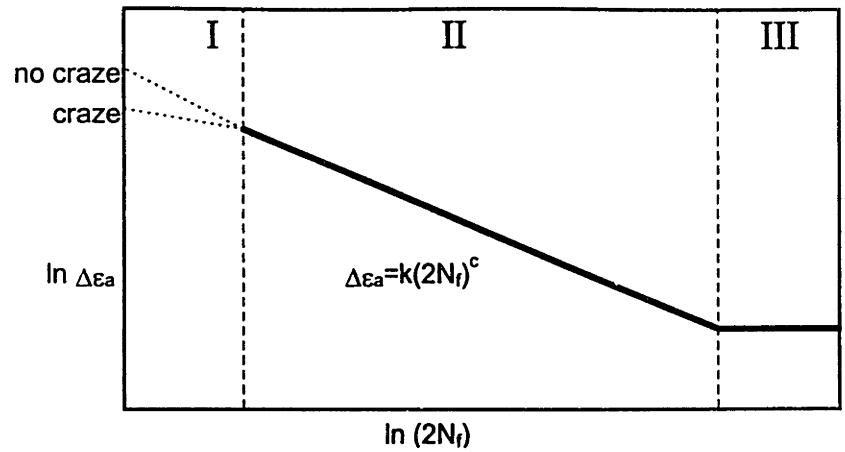

Figure 2-9: Form of Polymer Strain-Life (Beardmore & Rabinowitz 1975)

Present understanding of the mechanisms behind crack initiation in polymers is still incomplete, but higher molecular weight (Sauer, Foden, and Morrow 1977), lower cross-linking (Sauer, 1978), and greater crystallinity (Riddell, Koo, & O'Toole 1967) have been shown to correlate with longer fatigue life.

2.2.3 Cyclic Softening

As a test progresses, polymers invariably experience cyclic softening. At constant strain applied stresses will decrease. At constant stress, strains will increase. This effect can be exacerbated by thermal factors, but cyclic softening itself is entirely a mechanical material response. Unlike metals, polymers will never cyclically harden. (Beardmore & Rabinowitz 1975). Polycarbonate typically experiences a long period of cyclic stability in which the stress-strain behavior of the material maintains a new softer material state. This state is roughly 1% denser than the initial state and remains present when cycling has stopped. Some materials (such as ABS) experience continuous softening with no stable state. Others (such as PMMA, polypropeline, and glass fiber reinforced nylon) have no incubation stage and a subtle transition stage to produce an almost entirely stable stress level throughout cycling.

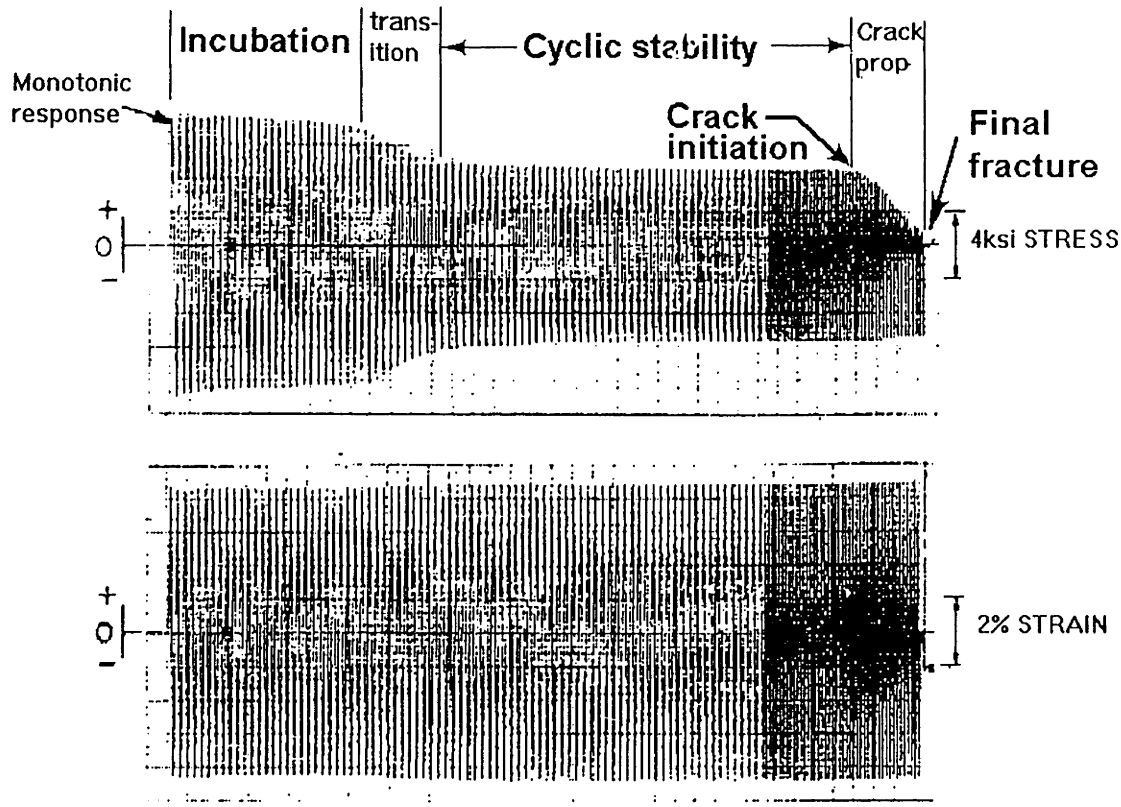

Figure 2-10: Time-series stress at constant strain (Beardmore & Rabinowitz 1975)

The increased density near the end is due to a change in recorder speed.

The incubation, transition, and stable regions can also be represented with stress plotted against strain in a traditional hysteresis curve plot as is shown in Figure 2-11:

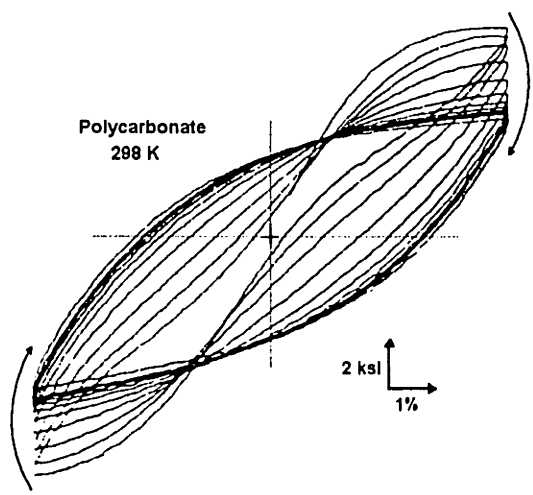

Figure 2-11: Cyclic softening of PC (Beardmore & Rabinowitz 1975)

2.2.4 Hysteresis Curve Shape & Properties

Polymer hysteresis curves display behavior rarely seen in metals, but tend to be similar enough to use the same fatigue theories. The initial propeller-like shape of the hysteresis curve in Figure 2-11 is the result of time-dependent flow mechanisms (Beardmore & Rabinowitz 1975). As cycling progresses and softening takes place, the hysteresis takes on the familiar almond shape, allowing the researcher to generate a traditional cyclic stress-strain curve as seen in Figure 2-12. Note that the maximum stress experienced during peak compressive strain ($\sigma_{c(max)}$) is greater in magnitude than the maximum stress experienced during peak tensile strain($\sigma_{t(max)}$). The ratio σ_c/σ_t is the same in the monotonic and cyclic stress-strain curves. This strength differential (or "S-D") effect is common in ductile polymers, (Beardmore & Rabinowitz 1975) which makes zero-mean strain-controlled cycling not directly comparable to zero-mean stress-controlled cycling.

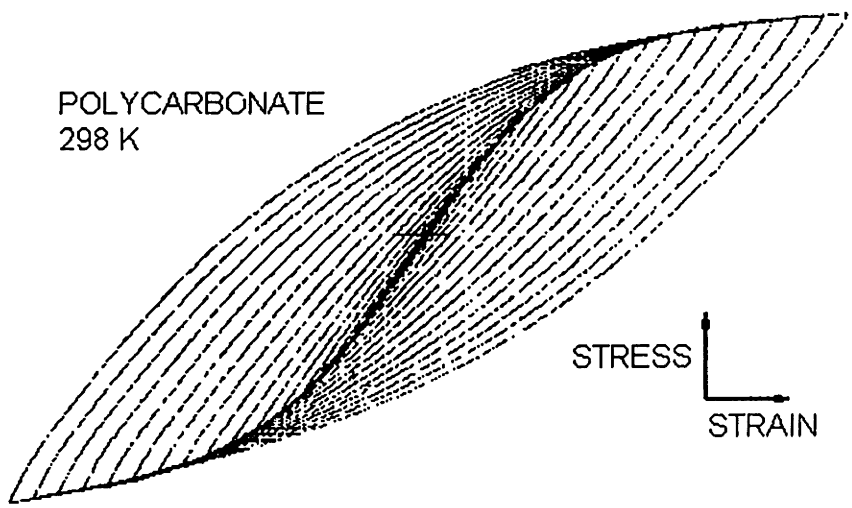

Figure 2-12: Polycarbonate stable-region hysteresis loops (Beardmore & Rabinowitz 1975)

The factor-of-two effect when generating the unloading curve from the cyclic σ–ε curve holds as well for plastics as metals. The following figure was generated from Figure 2-12 in the same manner as the steel in Figure 2-3:

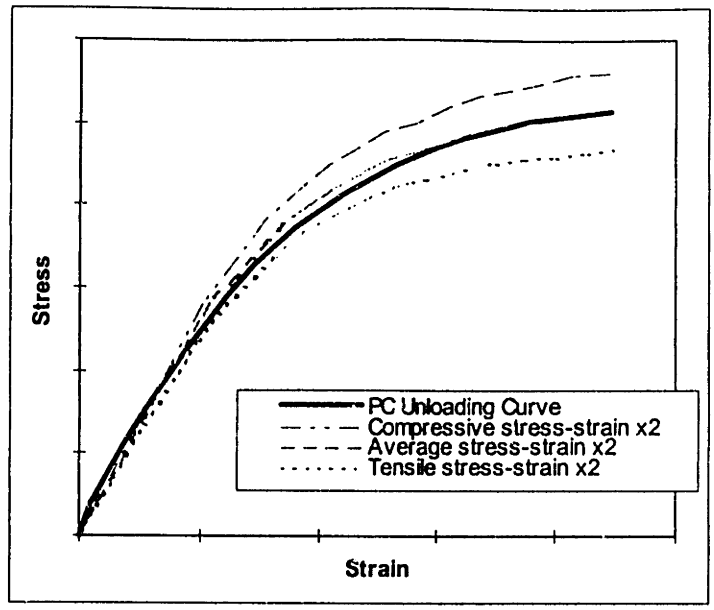

Figure 2-13: Factor-of-two unloading curve for PC (After Beardmore & Rabinowitz 1975)

Note that this plastic has a much greater difference between its tensile and compressive behavior (S-D effect) than the steel. The scaled average cyclic σ–ε curve is very close to the actual unloading curve.

Cyclic stress-strain curves typically exhibit behavior different from the monotonic curve.

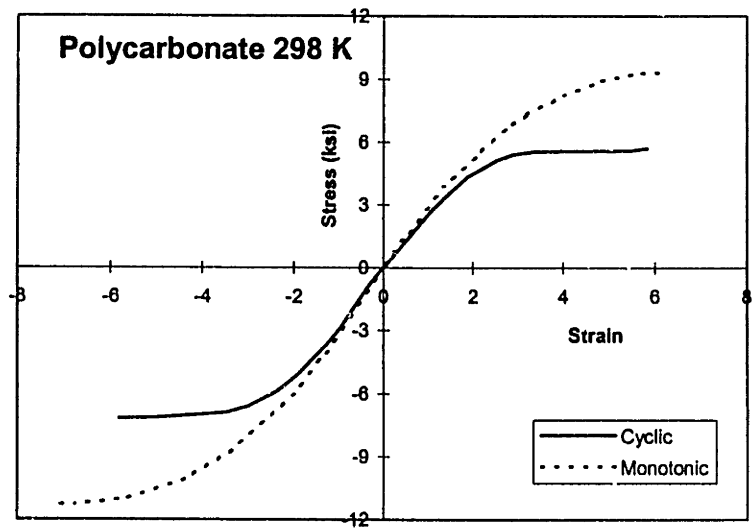

Figure 2-14: Cyclic/Monotonic σ–ε curves (after Beardmore & Rabinowitz 1975)

Both curves will usually be similar at low strains and exhibit the same linear-elastic response. The cyclic curve, however, usually diverges from the elastic line earlier and stabilizes at a lower stress.

2.2.5 PFLAP Modifications

In order to perform a fatigue life analysis on polymers, the existing FLAP code was altered. The original code relied upon Coffin-Manson fits to describe the strain-life curve. As was shown earlier, polymer strain-life curves rarely conform to the Coffin-Manson equation. Instead of relying on fits which assume a certain strain-life shape, the program was recoded to accept digitized points which form a strain-life curve. Strain levels below the minimum present in the strain-life lookup table were set to an (essentially infinite) life of 10^9 cycles. All other life levels were interpolated or extrapolated in log-log linear fashion from existing points. While this change added flexibility by allowing any strain-life form, it also prevented the program from using any of the mean stress correction theories.

PFLAP used an input file to describe the Ramberg-Osgood elastic-plastic stress-strain parameters and to contain the strain-life lookup table. The following is an example input file. The three numbers on the top line are K', n' and E (units KSI). The remaining lines each contain a data point consisting of a strain and a number of cycles to crack initiation.

```
11     0.08   300
0.0001        1.00E+09
0.003         300000
0.015         14000
0.025         2500
0.035         700
0.041         64
0.1           0.5
```

3. PHYSICAL TESTING

Testing consisted of four broad categories, each of which will be detailed in the following section.

1) Generating the strain-life curve for polycarbonate
2) Evaluating that material's agreement with Neuber's Rule
3) Evaluating the material's agreement with the Palmgren-Miner rule
4) Comparing a road-cycled component's actual and predicted life.

3.1 Material Characterization

The durability analysis program uses strain-life curves in order to predict the expected life of a given element experiencing a certain strain. The goal of this testing phase was to generate a strain-life curve for a commercial

grade polycarbonate. This material was chosen because it was present on a vehicle part which exhibited failure during cyclic loading. A different grade of polycarbonate was also studied by a different researcher (Beardmore & Rabinowitz 1975), allowing results to be compared.

3.1.1 Method

Testing was conducted on GE Lexan EM3110 (polycarbonate) specimen bars. Each bar was CNC machined at a slow feed rate from a 6x8" plaque with the grain longitudinal to the direction of loading. Standard dogbone tensile bars are often used for fatigue tests, but they buckle under compressive load and can be used with tension-tension testing only.

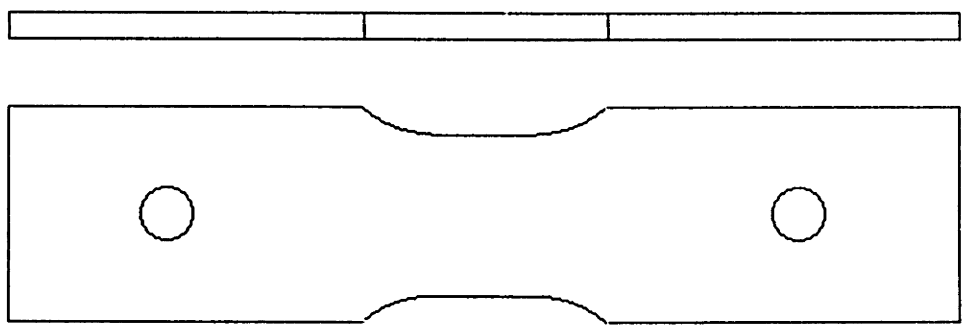

Figure 3-1: Fatigue test bar

Testing was conducted at room temperature (298 K) with a small number of points taken at an elevated temperature (343 K). Each temperature allowed the generation of one strain-life curve. Historically, polymers have displayed significant sensitivity to test conditions which results in large amounts of scatter in strain-life data. This is largely because test temperatures have been relatively close to the melting temperature (T_m) of the material. For a T_m of 408 K (GE Select, 1995), these test temperatures amount to a T/T_m of 0.72, and 0.87 respectively. In the region of $T/T_m>0.6$, metals display similar sensitivity and subsequent scatter (Skelton 1987).

All bars were tested in a fully-reversed compression-tension strain-controlled fashion. Strain controlled and stress controlled tests can produce very different results. Stress-controlled testing in the plastic regime is susceptible to

thermal and creep runaway, making strain-controlled testing the most useful method. Zero-mean tension-compression testing was chosen because it most accurately reflects the loading experienced by most parts.

A triangular waveform was used for all tests. This waveform has the benefits of a constant strain rate, crisper hysteresis curves, and a closer resemblance to road load inputs. In addition, a triangular form spends less time at peak strain amplitudes than a sine wave, reducing creep effects (Beardmore & Rabinowitz 1975). In the elastic region, waveform is not a critical factor in determining the life of the part. In the plastic region, waveform effects have been shown to influence fatigue life (Beardmore 1978).

Tests were conducted at 0.5 Hz in order to minimize the effects of hysteretic heating. In the case of low-strain tests, some samples were switched to load control with higher sinusoidal cycling frequencies after cyclic stabilization. Mechanical fatigue of polymers has been shown to be frequency insensitive. Thermal fatigue failure has been shown to be extremely sensitive to frequency effects (Crawford & Benham 1975). As long as thermal buildup is minimized, frequency effects should not affect the results to any great extent.

15 samples were used to define the room temperature strain-life curve. The highest tested strain range was 4.08%. Specimen buckling precluded testing with any greater zero-mean strain ranges. The lowest tested strain range was 0.3%. Two samples were tested at strain ranges of 0.8%, 1.0%, 1.5%, and 3.5% in order to gauge the repeatability of the test. Six data points were taken at the elevated temperature, ranging from 0.4% to 3.0% strain.

The definition of "failure" in a cyclic load situation can be very dependent upon the requirements of the material being tested - failure can be defined as a certain degradation of stiffness, load carrying ability, or even optical qualities. For the purposes of this test, "failure" was defined as the initiation of a crack. Crack initiation was considered to have taken place when the tensile stress carried at the constant strain level began to drop to zero while still maintaining compressive strength. (See Figure 2-10)

Additional "incremental" testing was conducted to provide greater detail to the cyclic stress-strain curve. Strain-controlled cycling was conducted at many different strain amplitudes and mean strains and the max/min stresses recorded.

Perhaps as important as a listing of test variables is a discussion of what was *not* tested. Since there is no mechanism-based method with which to generate a strain-life curve, families of curves must be generated for every variation in test conditions. It is impossible to characterize even one material for all possible variations in input. It was the goal of this test plan to generate the most useful data with a conservative use of resources. As additional minor factors begin to be considered, decreasing returns to effort dictate a sensible limit to the extent of testing.

3.1.2 Results & Discussion

The room temperature strain-life and stress-strain curves formed the core data set for the PFLAP program. The strain-life curve used by the program is the solid trendline of Figure 3-2. The solid line of Figure 3-3 is the result of a fit of the Ramberg-Osgood parameters to the cyclic stress-strain curve.

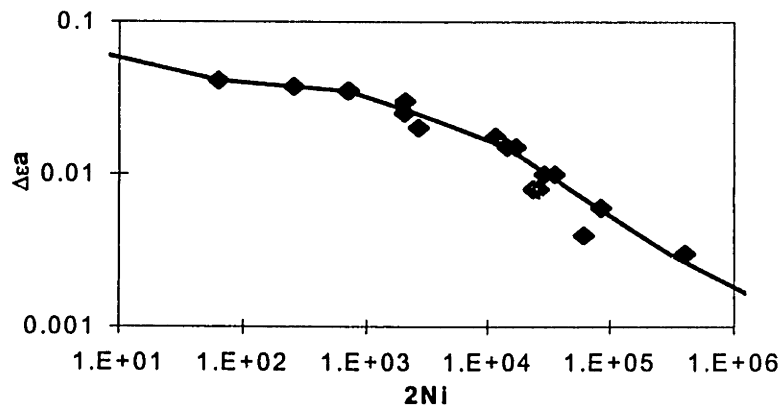

Figure 3-2: PC Strain-Life (?98 K)

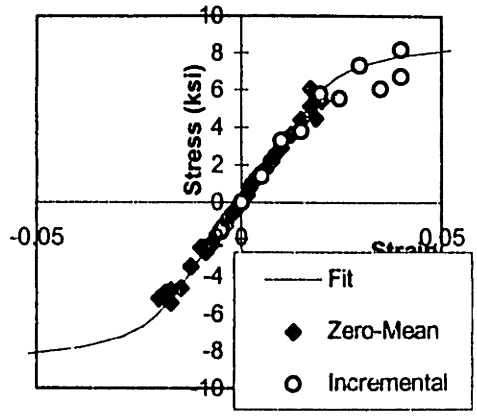

Figure 3-3: PC Cyclic Stress-Strain (298 K)

Most of the testing was conducted in the elastic regime. As soon as any plastic strain was introduced, life levels became very short. The incremental cycling tests were necessary to gain any useful knowledge of the cyclic stress-strain behavior in the plastic range.

Data taken from high-temperature testing shows slightly lower lives and softer stress-strain response than room temperature results. The two are plotted together in Figure 3-4 and Figure 3-5.

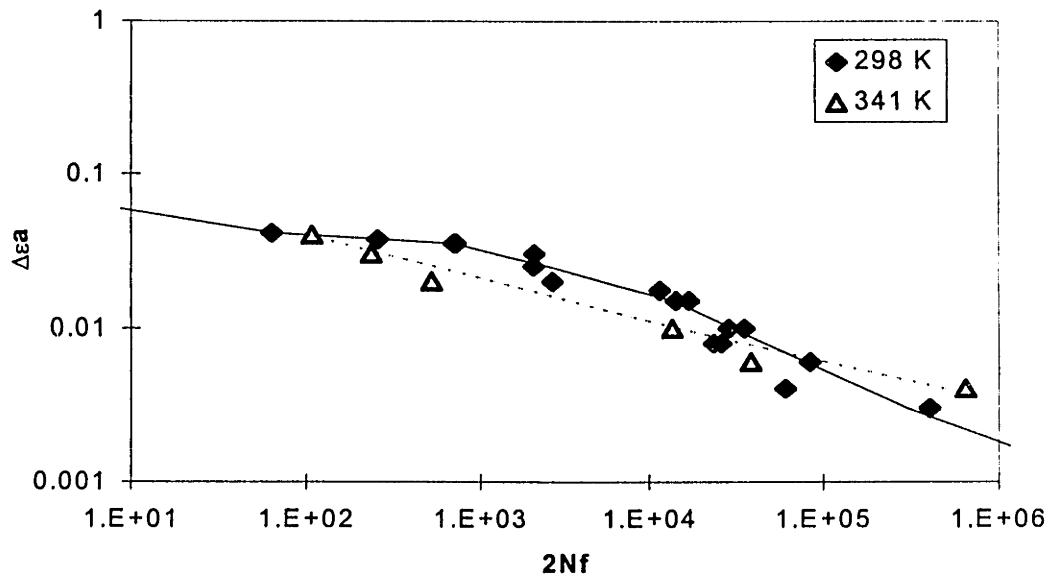

Figure 3-4: Elevated and Room Temperature Strain-Life

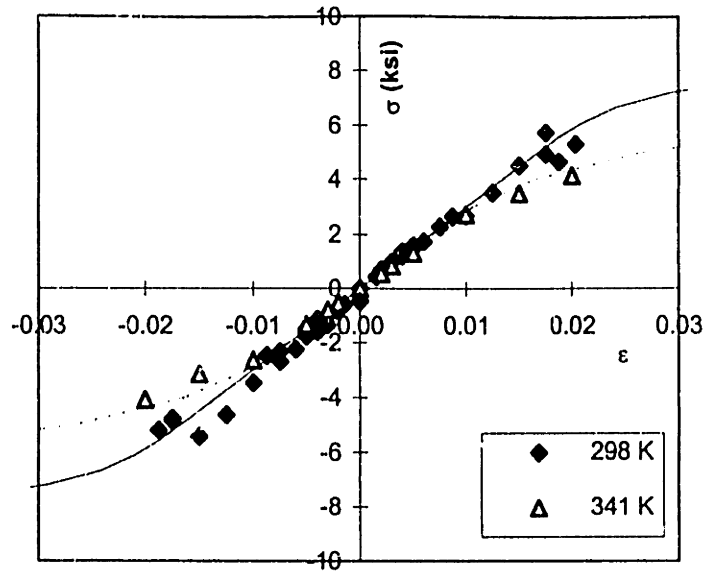

Figure 3-5: Elevated and Room Temperature Cyclic Stress-Strain

The elevated-temperature strain-life curve sits mostly within the scatter for the room-temperature data. The most important change caused by high temperature is the softening of the stress-strain curve.

All available test points show significant scatter. Four of the tested strain levels were conducted twice and show only small life differences between runs. This, however, masks the scatter implied by large life changes as a result of a negligible strain change and even the occasional *shortening* of life resulting from *lower* strain levels. This amount of scatter makes it difficult to draw a trendline which is useful as a PFLAP data set.

The present trendline was generated by drawing a nonparametric line which fit the points. It was then altered by making iterated changes to the line in an effort to reduce the "error" of the fit. "Error" in this case is defined by the average absolute percentage difference between a given strain's observed life and the life described by the trendline. The line which gave the best combination of a plausible shape and low error still resulted in an error of 35%. This means that all calculations based upon this fit line will necessarily have a minimum error of about 35%. This built-in error is a result of the widely scattered strain-life data.

The wide variety of polymer strain-life curve shapes demands a flexible fit to the data which is not bound by assumptions of the curve's form. The nonparametric nature of the fit allows this method to be used for many different types of polymers.

Sources of data scatter:

A significant amount of variation is introduced by the difficulty of detecting the initiation point - in almost all cases the plot of stress at constant strain showed only subtle degradation of tensile stress. Deciding on the exact initiation point was in many cases a judgment call which could easily vary across a wide range. Final failure life (which is not subject to a judgment call) also showed great scatter, so this can not be the sole source.

The most extreme examples of scatter in final failure life can be attributed to the differences between out-of-gage and in-gage failures. If the crack initiated within the region measured by the extensometer, the controller would decrease tensile loads after the formation of a crack in order to maintain a constant strain. This decreasing load would then slow crack growth and result in long life until total failure. If a crack initiated outside of the extensometer-measured region, the controller would increase load in order to maintain the same strain level. As each increased load grew the crack and caused measured strain to drop, load would continue to increase and grow the crack even faster, resulting in a fast run-out to failure. In theory, failure location should accelerate only the final failure life, not the initiation life. However, the samples which displayed an out-of-gage failure also tended to have much earlier initiation points. This suggests that initiation may actually occur very early in the life of the test bar. This initiation is undetectable by sole observation of the strip chart recordings because it does not have a dramatic enough effect on load levels.

Some of the scatter could simply be the result of extreme sensitivity to test conditions. As has already been discussed, when metals reach 60-70% of their melting temperature, small or imperceptible changes in test conditions can have significant effects upon life to crack initiation (Skelton, 1987). Steps were taken to insure that all tests were conducted in as similar an environment as possible, but conditions may have changed from test to test:

- The temperature of the lab may have changed by 2-3°K
- Different strain gages may have caused the controller to react differently
- The samples may have been slightly misaligned in the test machine
- Small machining imperfections may have made specimens not identical
- The material used may have been from different processing batches

The exact sensitivity of the sample to these varying factors is not known.

These results can be compared to two different existing data sets. Beardmore & Rabinowitz (1975) tested a different form of polycarbonate under nearly identical conditions. The material's manufacturer (GE Select 1995) provided fatigue data on the same material (Lexan EM 3110) but under different test conditions.

Beardmore & Rabinowitz (1975) tested a polycarbonate which was ductile at room temperature - the Lexan displayed more brittle behavior. The strain-life curve shows a Type I "kink" typical of more brittle polymers which is explained by visible crazing during high-strain cycling. Beardmore & Rabinowitz's polycarbonate displayed incubation, transition, and stable regions as shown in Figure 2-10. The Lexan showed no incubation and remained mostly stable in its stress range until initiation.

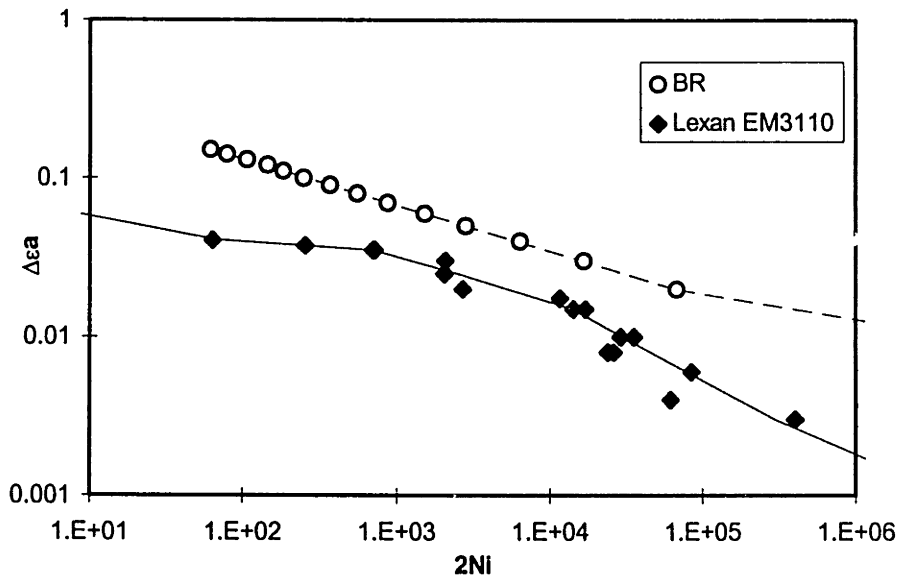

Figure 3-6: Comparison with Beardmore & Rabinowitz (1975)

The material's manufacturer provides fatigue data (GE Select, 1995) from a tension-tension load-controlled test. Instead of initiation, this data is presented as the number of cycles to total failure of a 0.5 inch wide Type I tensile bar. Due to the high frequency of testing, it is possible that some recorded failures may be the result of thermal run-out instead of mechanical fracture. Since cyclically stabilized stress amplitudes and final failure points were recorded for the strain controlled testing, it is possible to compare the results of the two data sets.

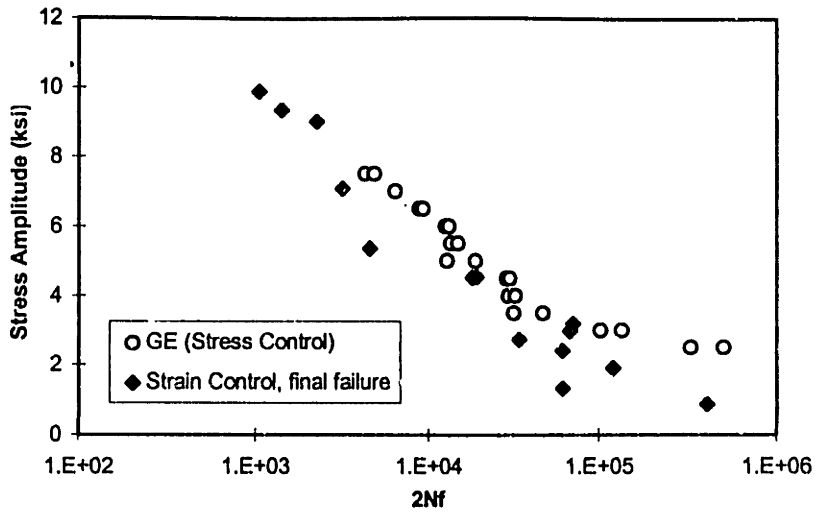

Figure 3-7: Stress and Strain Control to Final Failure

The data shows the unexpected result that the GE data indicates slightly longer life at a given stress level. Due to the higher mean stresses imposed by tension-tension testing, the GE data should show comparatively lower lives for the same stress amplitude. Note also that the number of propagation cycles from initiation to failure should be lower in the GE data since the sample bar is narrower. Load control will also increase the stress on the remaining ligament after initiation, causing faster propagation than strain control which will decrease stress on the ligament after initiation.

This discrepancy could be the result of different additives. The test bars used for the strain-controlled tests contained black pigmentation. The manufacturer's data shows results from the material in its natural state with no color additives. It is possible that the color additives could degrade the fatigue properties of polycarbonate.

Another explanation involves the surface finish of the samples. The manufacturer's data is generated from smooth-sided injection molded samples with continuous molecular chains and defects no larger than those of the mold. The samples used in the strain-controlled testing were machined from a blank and probably contained broken molecular chains at the edges and surface defects from the mill bit. These small defects could provide local stress risers which would later become initiation sites.

The manufacturer also provides a monotonic stress-strain curve at room and elevated temperatures (GE Select 1995). This allows the comparison of the monotonic and the tensile portion of the cyclic stress-strain curve for both temperatures.

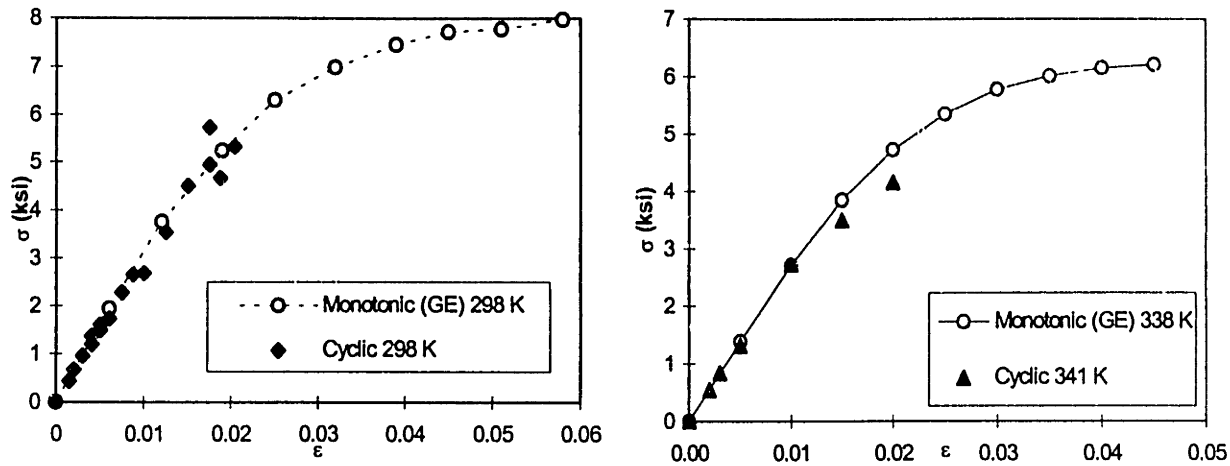

Figure 3-8: Monotonic/Cyclic Stress-Strain Curve Comparisons

The cyclic stress-strain curves display behavior which is close to that of the monotonic curves. This behavior is unusual - most polymers show distinctly softer behavior in the cyclic curve. A possible explanation for this is that little of the fatigue testing actually entered the plastic range - differences would certainly be more noticeable at higher strain levels.

3.2 Smooth and Notched Bar Incremental Cycling

The purpose of this testing stage was to evaluate the validity of Neuber's rule for the polycarbonate. Neuber's rule is used in PFLAP to transform linear-elastic FEA predictions into elastic-plastic stress and strain results.

3.2.1 Method

This testing was conducted in the manner of Conle (1977). An incrementally increasing cyclic load history was run through two different types of notched specimens (Figure 3-9). Three specimens of each type were tested in this manner. Instead of an extensometer measuring strain in the gauge section, a strain gauge was placed in the notch to measure local strain. This local strain was then plotted against the far-field net-section nominal stress.

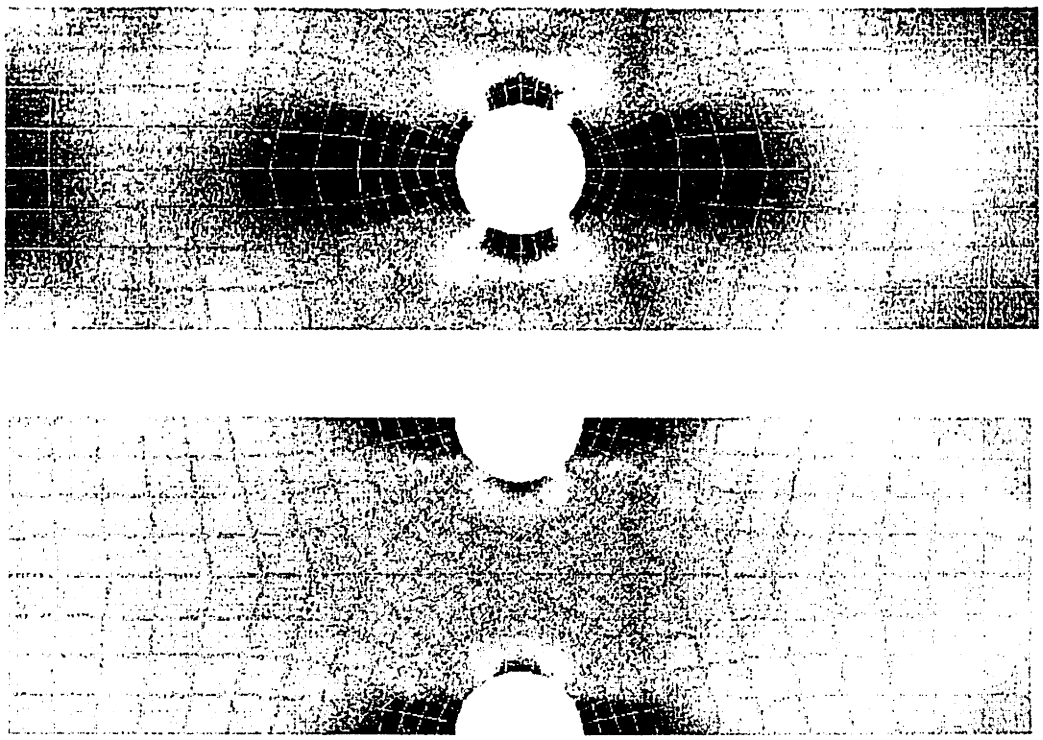

Figure 3-9: Coarse-Mesh FEA Center Hole and Edge Notch Specimens

Stress concentration factors (K_t) at the notch tip were approximated using reference materials (Tada 1985), then determined using a fine-mesh finite element analysis. K_t was calculated as the ratio of the maximum stress at the notch tip divided by the far-field stress. This analysis was repeated with increasing element density in the notch until K_t values converged.

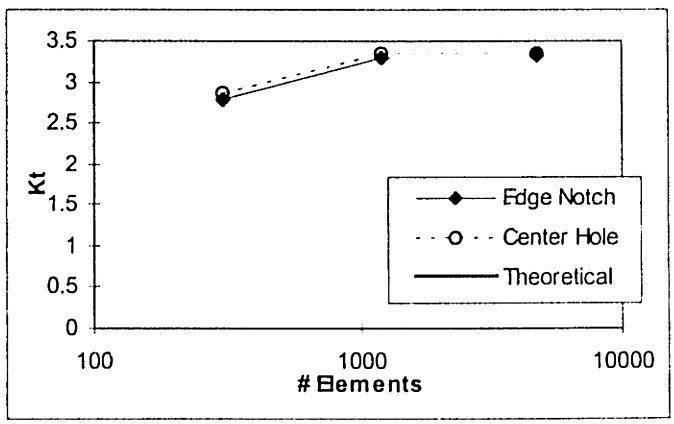

Figure 3-10: Concentration Factor Convergence

3.2.2 Results & Discussion

From the testing conducted in section 3.1, it is possible to generate a ΔS-$\Delta\varepsilon$ curve for the smooth-sided specimen by multiplying the $\Delta\sigma$ by the ratio of A_{min}/A_{max} (The cross sectional area of the thin portion divided by the cross-sectional area of the gripped portion.) This can be compared to the ΔS-$\Delta\varepsilon$ curve of the notched specimens.

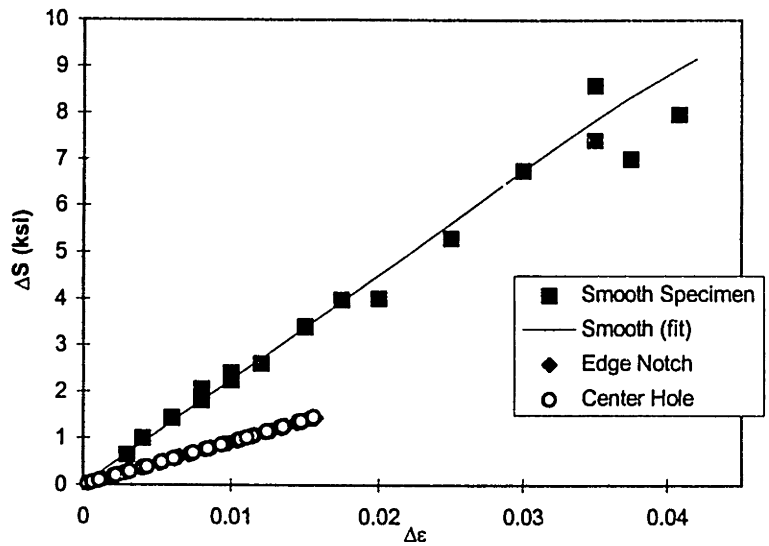

Figure 3-11: Nominal Stress vs. Strain for Three Geometries

The notched samples were only tested to very low strain amplitudes. The samples buckled at low load amplitudes, limiting the testable range. Stress-strain response in this limited range was very linear. Monotonic testing on identical samples showed that in both cases yield did not occur until nominal stresses in excess of 5 times greater than the range tested here were applied. This testing therefore took place almost entirely within the elastic portion of the material's stress-strain curve.

There was a high degree of repeatability within both geometries' three sample curves. This is probably due to the low load amplitudes tested - notice that the smooth specimen did not display unusual behavior until it entered high strain amplitude testing.

Both notched specimens had similar nominal stress-strain response. This is to be expected given their identical stress concentration factors and cross-sectional area.

Given the stress concentration factor in each specimen's notch, the notched ΔS-$\Delta\varepsilon$ curves, and a $\Delta\sigma$–$\Delta\varepsilon$ curve, it is possible to quantify the effectiveness of Neuber's rule for the material. Each strain amplitude ($\Delta\varepsilon$) has a corresponding real stress amplitude ($\Delta\sigma$) determined from the smooth specimen and a corresponding nominal stress amplitude (ΔS) determined from a notched specimen. The full form of Neuber's rule allows these two stresses to be compared based upon the K_t of the geometry. (This factor of K_t is removed in PFLAP because the finite element analysis is left to calculate geometric effects.) Taking the full form of Neuber's Rule $\Delta\sigma\Delta\varepsilon=K_t^2\Delta S^2/E$ (Seeger & Heuler 1991), we see that we can evaluate the rule by plotting true stress and strain against the stress concentration factor times the nominal stress and strain.

Such a graph is presented in Figure 3-12 for both specimens. The closer the results are to the 45 degree line, the better Neuber's rule applies to the material. Points found in the lower right diagonal of the graph indicate a conservative prediction, those in the upper left show a nonconservative result.

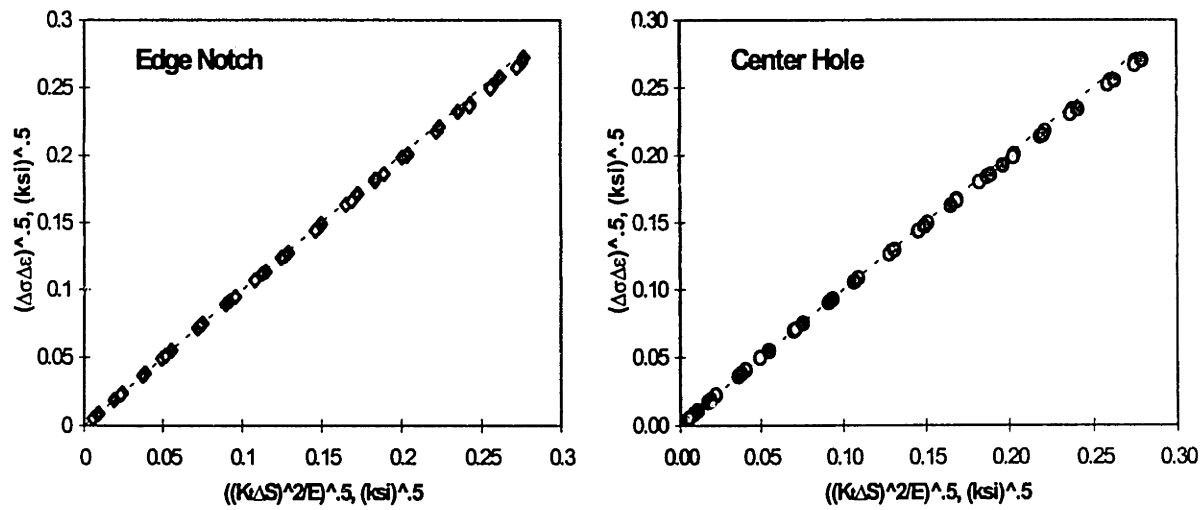

Figure 3-12: Neuber Comparison Result - Edge Notch and Center Hole Geometires

Both samples displayed behavior very close to the Neuber prediction line. This is not surprising since the samples remained mostly elastic during testing. Neuber's rule serves only to approximate elastic-plastic response from a linear calculation. With no data representing the plastic regime, Neuber's rule does not have a significant effect upon these samples. For this reason there is no clear conclusion regarding the effectiveness of Neuber's rule in this polycarbonate.

A similar procedure was followed by Conle (1977) and produced Figure 3-13:

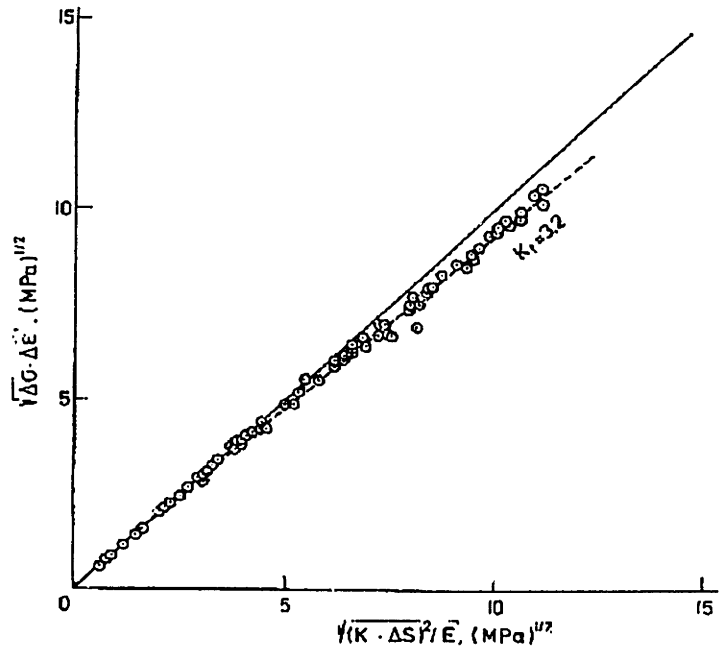

Figure 3-13: Neuber's Verification for Aluminum (Conle 1977)

Conle's data shows similar scatter to the notched polymer samples, but has a larger deviation from the Neuber prediction. This is mostly due to the fact that Conle's data actually enters the plastic regime, whereas the polymer test samples remained mostly elastic during cycling.

Neuber's rule was originally derived for prismatic bodies acting in pure shear. Violation of these assumptions will produce a conservative result (Tipton 1991).

The mounting of the strain gages in the small notches may have introduced error unrelated to the effectiveness of the theory. Misalignment of the gages would have caused strain amplitudes to go underreported, referencing the recorded nominal stress with a lower true stress. This would cause results to err even greater to the side of conservatism.

3.3 Test Bar Variable Strain Cycling

Real-life loading rarely occurs at a constant strain amplitude, necessitating some estimation of life at varying combinations of strain levels. The Palmgren-Miner cumulative damage rule assumes a linear accumulation of

damage and has proven to be effective for metals. The goal of this phase of testing was to investigate the applicability of the Palmgren-Miner rule to polycarbonate.

3.3.1 Method

2-Step Tests

The test bars shown in Figure 3-1 were cycled in strain control at a high (3.5%) and a low (1.5%) strain level. A variety of tests were run in which the bar was cycled for a set number of cycles at one level, then switched to the other level and let run until a crack initiated. Samples were started at both the high and low strain levels and allowed to run for varying percentages of the expected constant-strain life before switchover to the new strain level. (See Table for details)

	Step 1			Predicted Step 2		
Test #	Δεa1	n1	n1/N1	Δεa2	n2	n2/N2
28	1.5	3100	0.20	3.5	560	0.80
29	1.5	6200	0.40	3.5	420	0.60
30	1.5	9300	0.60	3.5	280	0.40
31	1.5	9479	0.61	3.5	272	0.39
32	3.5	145	0.21	1.5	12289	0.79
33	3.5	117	0.17	1.5	12909	0.83
34	3.5	430	0.61	1.5	5979	0.39
35	3.5	40	0.06	1.5	14614	0.94
44	1.5	1550	0.10	3.5	630	0.90
45	1.5	3100	0.20	3.5	560	0.80
46	1.5	4650	0.30	3.5	490	0.70
47	3.5	70	0.10	1.5	13950	0.90
48	3.5	140	0.20	1.5	12400	0.80
49	3.5	210	0.30	1.5	10850	0.70

Table 3-1: Two-Step Damage Accumulation Plan

Load History Tests

Test bars were also cycled with a complicated load history typical of vehicle inputs. Different histories were artificially constructed to allow evaluation of a range of cycling types. Each file was constructed by summing a frequency spectrum, multiplying the resulting history, adding a mean load, then cutting off at upper and lower bounds. Load files were filtered to remove duplicate or intermediate load points.

Figure 3-14 shows the first 7 histories and the predicted most-stressed-element strain histogram for a single pass of the file. These files specified tension-tension cycling.

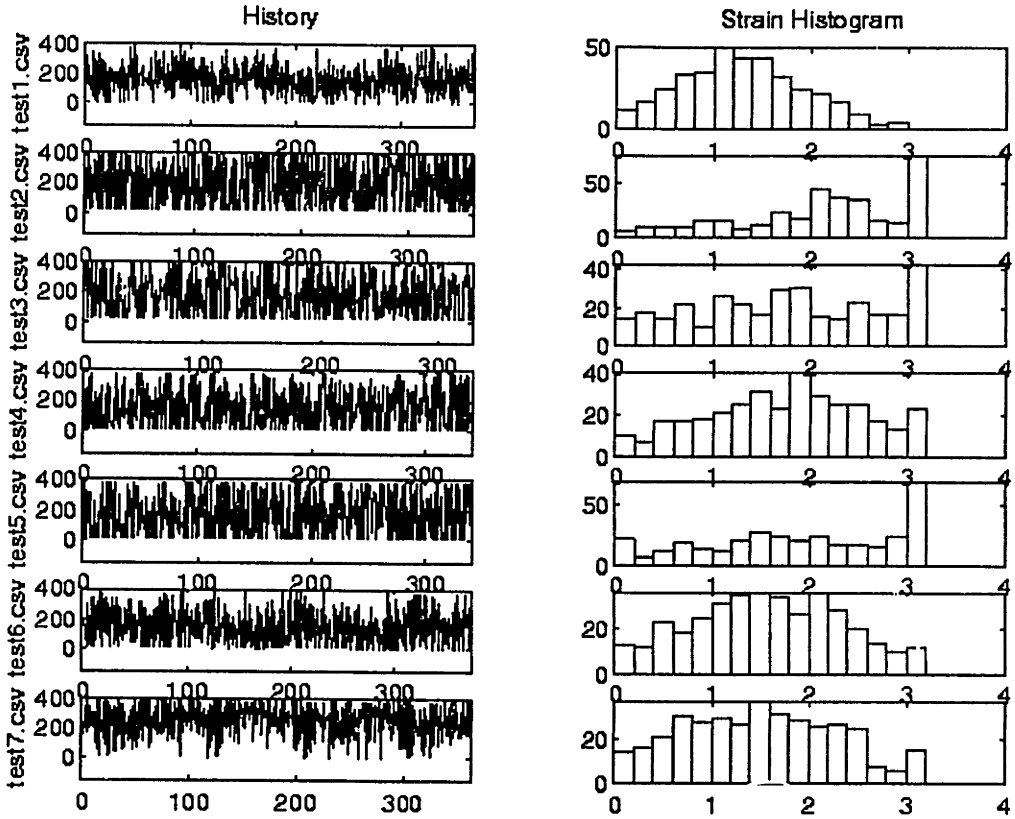

Figure 3-14: Load Histories 1-7

Input files 1-7 were purely tension-tension and were meant as a worst-case evaluation of the program's abilities. Test 7 in particular cycled mostly in the upper limit of the bar's tensile load carrying ability. Different distributions of load amplitudes and resulting strain ranges allowed these tests to have a wide variety of predicted cycles to failure. Input file test4 was conducted twice in order to evaluate the repeatability of the test.

Figure 3-15 shows the final 4 histories and the predicted most-stressed-element strain histogram for a single pass of the file. These profiles were conducted in tension and compression.

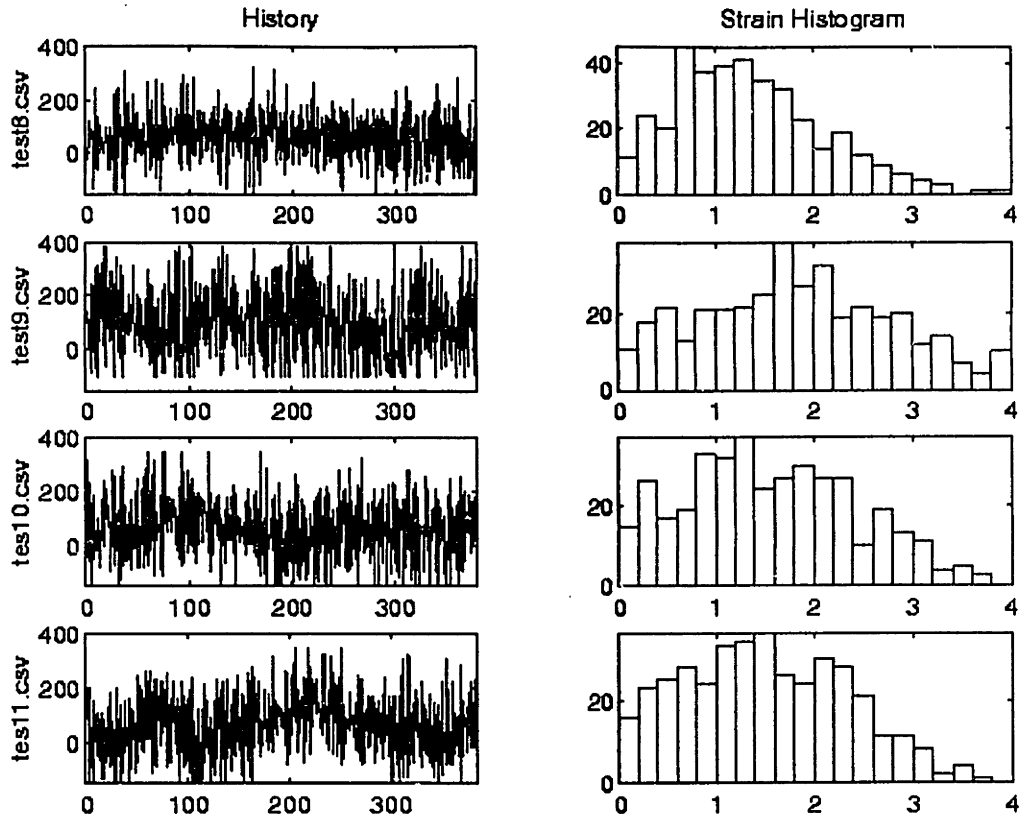

Figure 3-15: Load Histories 8-11

Input files 8-11 were intended to be more representative of vehicle loading, which is usually closer to zero-mean. These tests included a compressive component, but the maximum compressive magnitude was lower than the maximum tensile magnitude in order to prevent specimen buckling. The load patterns were varied in order to test at different expected lives.

	max load	min load	mean load	σ load	predicted 2Ni
test1	396	8	165	99	9325
test2	400	20	197	150	2702
test3	400	20	180	140	3658
test4	380	10	157	131	4285
test5	380	10	171	147	2952
test6	380	10	150	118	5490
test7	380	10	247	112	5735
test8	325	-150	62	103	6169
test9	350	-150	106	139	2044
tes10	350	-150	61	121	4354
tes11	350	-150	64	120	5234

Table 3-2: Test Bar Load History Properties

All tests were conducted at room temperature with one reversal every 1.5 seconds. The low cycling rate was necessary to allow the controller to reach the required load levels accurately and to prevent hysteretic heating. Test bars were monitored and visually inspected for crack initiation after every other load history file repetition. Since most files were 330-370 reversals long, an initiating crack could potentially have existed for about 350 cycles without being noticed. In practice, telltale signs of impending crack formation (such as dimpling and surface roughness) allowed more frequent inspections near the actual initiation. Since visual determination of an initiating crack involves a certain amount of judgment on the part of the inspector, it should be noted that predictions were calculated *after* the tests were conducted.

Modeling Details

The PFLAP program was used to generate life predictions based upon these load histories. The program used the solid trendlines from Figure 3-2 and Figure 3-3 as its strain-life and elastic-plastic stress-strain input curves. A quarter-bar symmetric model was developed to generate linear-elastic FEA results.

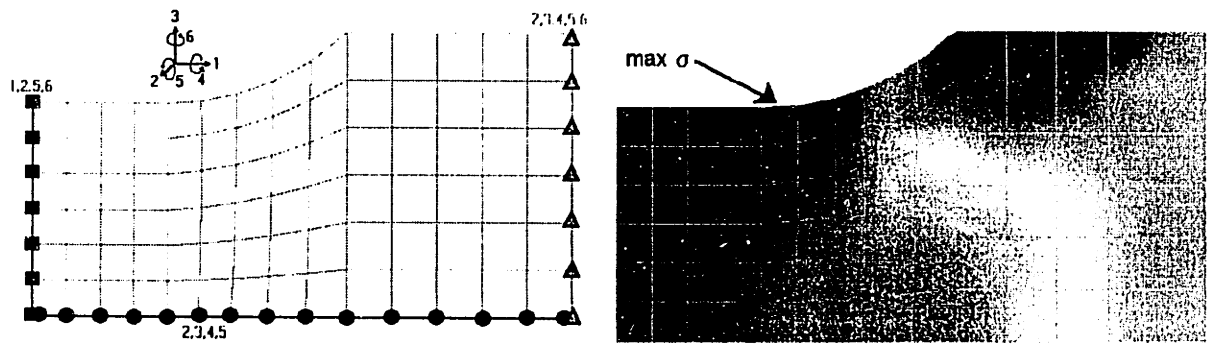

Figure 3-16: 1/4 bar model - mesh and static stress distribution

The linear-elastic model used the cyclic (not monotonic) stiffness and a Poisson's ratio of 0.308. Only 1/4 of the bar was modeled in order to take advantage of part symmetry and reduce computational time. Static analysis showed that the largest stress concentration typically took place at the narrow end of the radius. This is where most cracks were observed to develop during the strain-life testing.

3.3.2 Results & Discussion

The following graph plots the cycle ratios[1] of the low and high steps for the two-step tests. When using the Palmgren-Miner damage accumulation law, the cycle ratio is assumed to be equal to damage. In the following graph, any point directly on the dashed line has a summation factor of 1.0 and conforms to the Palmgren-Miner prediction. Any points to the lower left of the line indicate a summation factor <1.0 and have a life shorter than that predicted by Palmgren-Miner. Similarly, any points in the upper right diagonal have a summation factor >1.0 and represent a conservative underestimate by Palmgren-Miner.

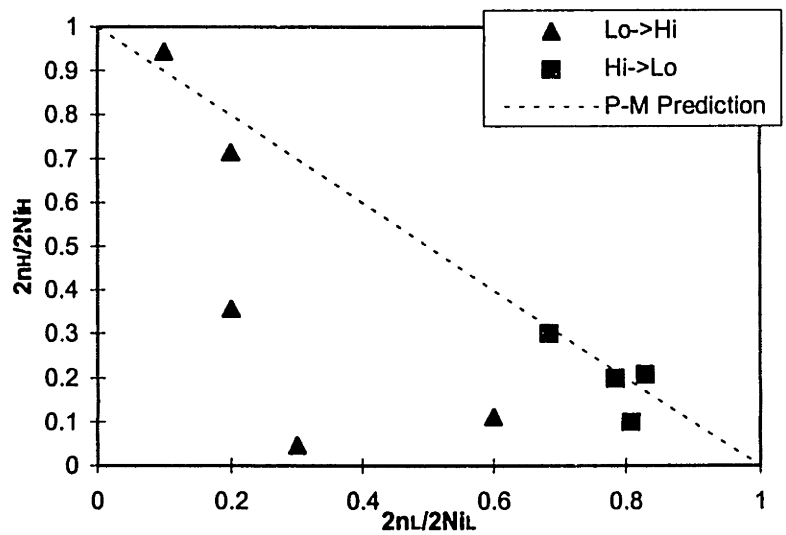

Figure 3-17: 2-Step Damage Accumulation

Collection of this data was significantly complicated by a great amount of scatter in simple constant-strain cycling. Some samples actually displayed initiation before the transition point. The hydraulic system in the test machine would often cause a compressive strain spike upon switchover from a low to a high strain level which would cause samples to buckle and fail. The results shown on the plot above are limited to those which survived both stage I cycling and the switchover to stage II. It is possible that the early failures of the two most extreme Lo->Hi points were the result of damage incurred from the strain spike during switchover.

---

[1] A cycle ratio is the ratio of number of cycles experienced to the number of cycles to initiation. A summation factor is the total of all cycle ratios.

It is typical for most Lo->Hi estimates to fall in the conservative range and for Hi->Lo estimates to be nonconservative (Miller & Zachariah 1977). This is mainly the result of nonlinear damage accumulation. It is not clear if the polycarbonate fits this theory. The Hi->Lo tests were on both sides of (but close to) the prediction line. The Lo->Hi tests gave nonconservative results, exactly the opposite of what would be expected. This is probably an indication that the use of a nonlinear damage accumulation rule would not improve the accuracy of P-FLAP's predictions.

Miller & Zachariah (1977) performed similar testing with mild steel at several different low and high strain levels. Since compliance with Palmgren-Miner decreases with increasing differences in strain amplitudes, it makes sense to compare test results with those which display a similar gap in expected life. $2Ni_L/2Ni_H$ for the polycarbonate testing was 15500/725=21.3. The closest test from Miller & Zachariah (1977) had $2Ni_L/2Ni_H$ = 16000/760 = 22.2

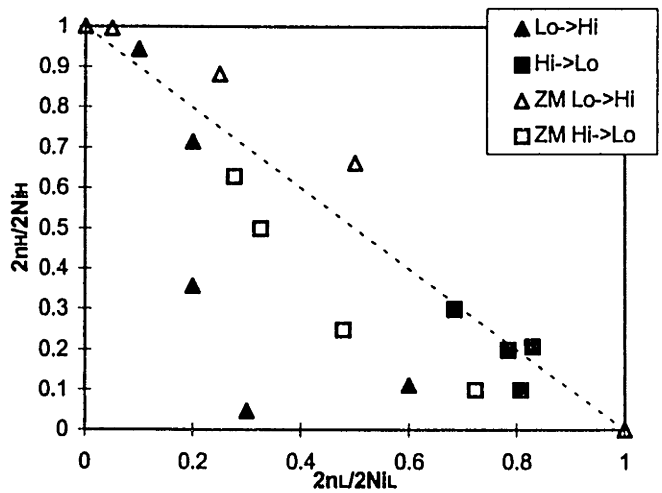

Figure 3-18: Two Step Comparison with Steel (Miller & Zachariah 1977)

With the exception of the two most extreme Lo->Hi tests and all of the unplotted data points, the polycarbonate and steel results seem to show roughly the same magnitude of agreement with the Palmgren-Miner rule.

Figure 3-19 shows a comparison of actual and predicted values for load history tests 1-11.

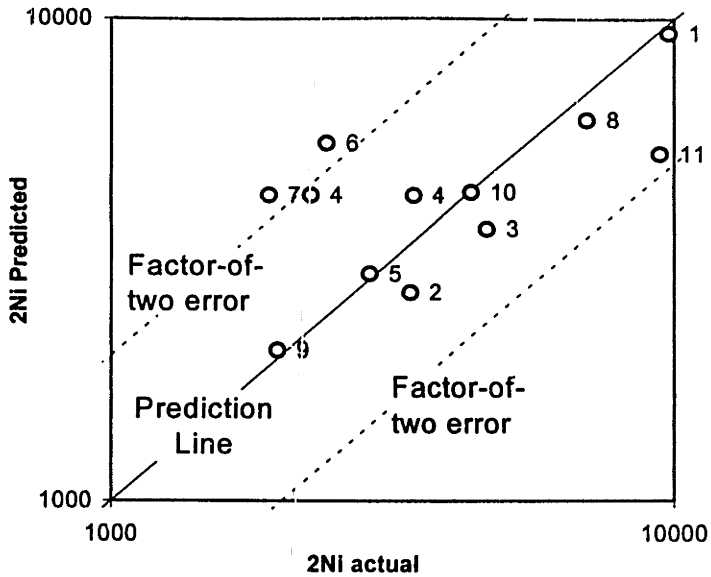

Figure 3-19: Load History Results: Test Bar

The immediate conclusion to be drawn from the random cycling data is that PFLAP usually predicts close to the actual number of cycles to initiation experienced under a complex load history. Eight of the tests were very close to the prediction line, and four were roughly a factor of two from the prediction.

History 4 was conducted twice in order to gauge the repeatability of the test. The result of the second test was significantly lower than that of the first. The difference between the two was a significant 41%[2]. This rather dramatically recreates the large scatter effects observed in the constant-amplitude tests.

History 7 was constructed to display unusually severe mean stress effects. Its peak stress was very close to the monotonic failure stress and most of the reversals took place within the top 30% of the load range. The program gave an extremely nonconservative result - just outside the factor-of-two range.

The tension-compression tests (8-11) gave encouraging results. Predictions were either very close to the prediction line (8-10) or conservative (11). Results from these tests are especially important since they are most representative of a typical vehicle load history.

---

[2] The percentage difference was calculated with respect to the average of the two lives.

Figure 3-20 shows an overall comparison of actual and predicted values for the 2-step and load history tests. Note that plotting full actual life and predicted life will cause Hi->Lo predictions to seem much less accurate than Lo->Hi tests since the overwhelming majority of cycling for the latter is merely defined as part of the test procedure.

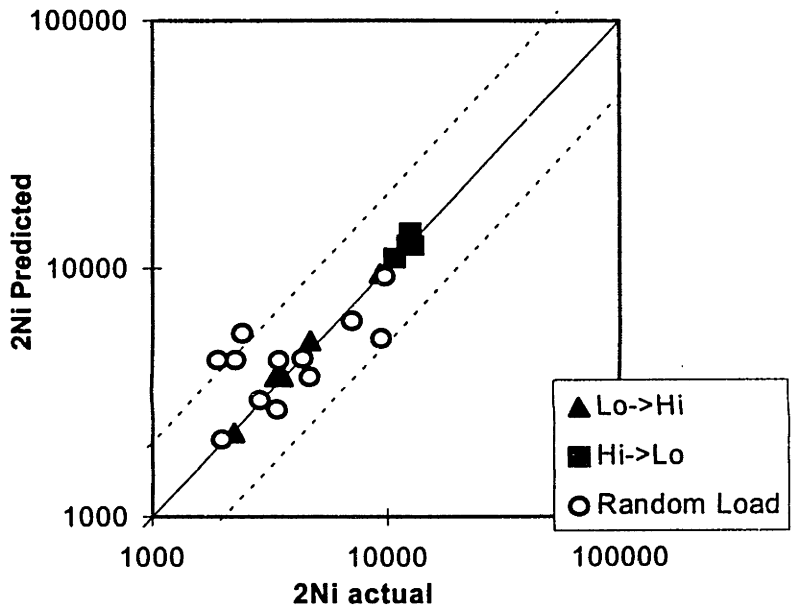

Figure 3-20: Prediction Quality, Test Bar

Deviations from predicted values can be the result of any number of factors. This stage of testing was conducted primarily as an evaluation of the effectiveness of the Palmgren-Miner damage accumulation rule. However, the presence of other factors makes it difficult to pin all error upon the damage accumulation law.

Much of the error shown could be the result of natural scatter. Even two seemingly identical samples in apparently identical test conditions cycled at the same strain amplitude can produce very different cycle lives. The importance of scatter can be seen in the samples which initiated a crack before switchover - since all testing was conducted at a constant strain range there could not possibly be any damage accumulation effects influencing the result. Since Palmgren-Miner relies upon a certain life at a certain strain range, significant error could result merely from the difficulty of estimating life under simple cyclic loading. The rule can only be as reliable as the data upon which it is based.

PFLAP does not consider mean stress effects, referencing all expected initiation lives from a strain-life curve generated with equal tensile-compressive cycling. This implies that the life referenced from the curve is probably

not the "true" life for a particular strain range and mean stress. Figure 3-21 plots each load history's mean stress versus the ratio of predicted/actual cycles to initiation. It shows a general trend toward more conservative predictions for histories with lower mean stresses. Load histories with small to moderate mean stresses resulted in actual lives close to or greater than predicted values. This implies that mean stress effects are probably not significant except in the most extreme cases.

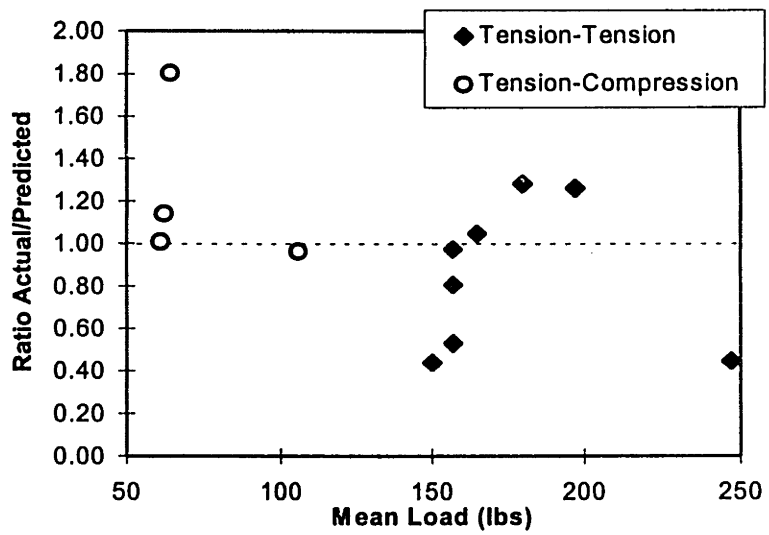

Figure 3-21: Mean Stress Effects and Prediction Quality

Some error could result from the test equipment's control mechanism. The controller was directed to reach the desired load for each reversal as quickly as possible, then proceeded to a new load after a fixed time interval. This would sometimes result in overshooting the desired load level. The actual load history experienced by the part could therefore be more severe than the control sequence used by PFLAP to produce the prediction. Observation of instantaneous load cell readouts indicates that this overshooting error was rare and seldom exceeded 3% of the desired amplitude.

In standard load history cycling, error could result from an inaccurate transformation from the input force amplitudes to the part's strain amplitudes. Fortunately, the relationship between zero-mean load and strain amplitudes was explicitly known for this part, allowing this module of PFLAP to be bypassed.

Given these and other complicating factors, it is difficult to determine exactly how much error actually derives from deficiencies in the damage accumulation rule. Average error in predicted vs. actual cycle lives for histories 1-11 is

40%. This is only slightly greater than the inherent 35% error which results from simple strain-life data scatter. This implies that strain-life scatter dominates any deficiencies in the damage accumulation law. This analysis is confirmed by the fact that the two-step tests seemed to randomly cluster around the Palmgren-Miner line instead of displaying any consistent bias. Therefore, Palmgren-Miner rule seems to provide an adequate measure for the summation of damage for complex strain histories in polymer parts.

3.4 Component Test

A polycarbonate tab on a commercial van has been shown to fracture after simulated road loading. This part was selected as a test case to insure that the durability method will work for realistic parts in realistic loading conditions.

The tab is part of a console bin which attaches to the engine cover. Three locator pins constrain the bin in five axes, leaving the tab to carry tensile/compressive loads in the "z" direction. The tab is held to the engine cover with a flexible steel "rollover clip" which allows the introduction of bending modes during axial loading. Figure 3-22 shows deformed and undeformed modes of a portion of this bin. The actual bin was cut to this portion during testing to simplify mounting into a load frame. Since the distant boundaries do not have much effect on local stresses in the tab this is still a realistic simulation of stresses experienced by the part.

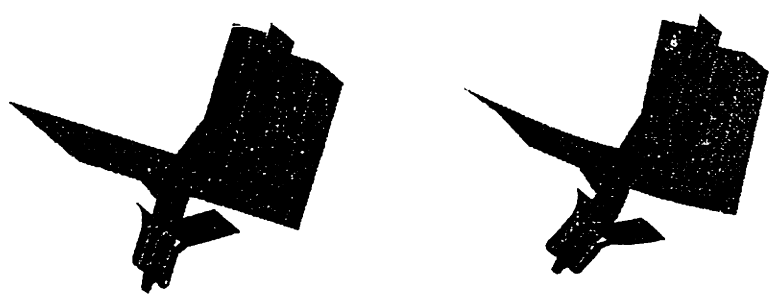

Figure 3-22: Console Bin Tab, Undeformed and Tension-Deformed

The polycarbonate tongue fatigue fractured roughly halfway into complete instrument panel simulated-life testing. This allowed the console to translate freely and produce shaking so severe that the console had to be removed in order to allow the test to continue. Since this part is not exposed to sunlight, lubricants, or paint the fracture was almost certainly a result of mechanical fatigue and not chemical attack. It is not known exactly when the tab fractured or when the fracture initiated during full-scale durability testing.

This stage of testing sought to replicate the loading experienced by the console bin in a controlled manner, then predict life and compare it to actual test results.

3.4.1 Method

The bin was made from Lexan EM3110. It was cut so that only the relevant high-load sections were included in the test. The rollover clip was attached as it would be in the vehicle and a fixture was bolted to the rollover clip in order to allow realistic boundary conditions. The top of the cut bin and the fixture were gripped in a uniaxial load frame, replicating the constrained movement of the bin in the van.

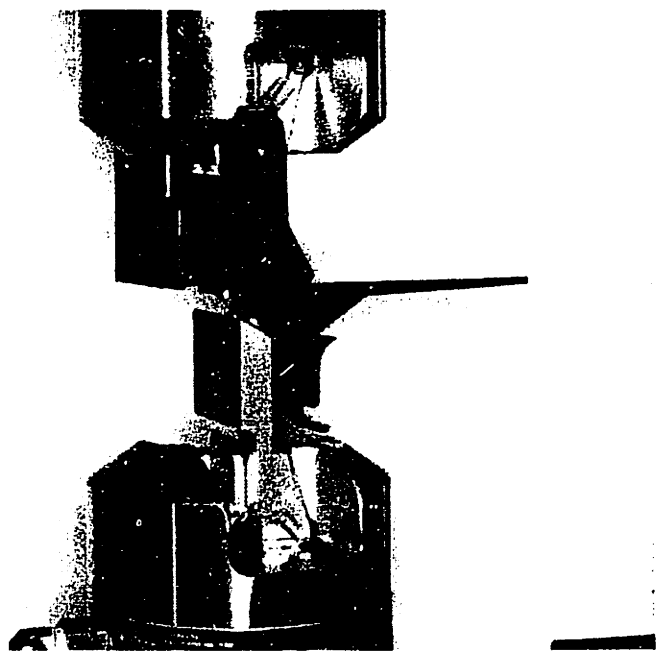

Figure 3-23: Tab Cycling Test Setup

Instead of load histories, the tabs were tested with a stroke history. The extremely soft response of the system and the small amount of slop at the tab/clip interface made it difficult for the controller to find the proper load accurately within a reasonable time. Desired load histories were generated using the same method as for the test bars. These load profiles were transformed into a stroke history by using a force-displacement curve[3] (as shown in Figure 3-24).

[3] The force-displacement response was almost entirely elastic, but a hysteresis effect appeared in the center region of the curve due to the relative motion allowed between the tab and the clip.

The stroke history was run through the tab/clip system and loads were recorded. The actual recorded load history was then used by PFLAP to generate a life prediction.

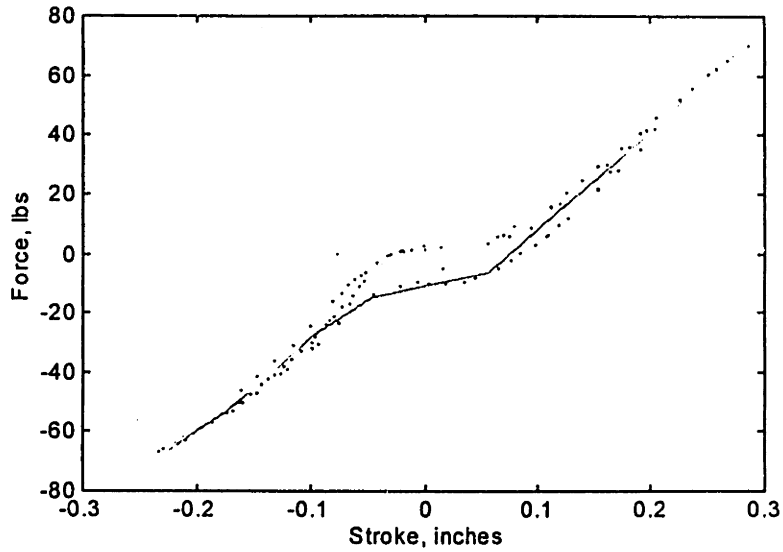

Figure 3-24: Tab Force-Displacement Curve

Displacements were specified in order to induce loads in the tab which were representative of worst-case real-world usage. Road testing recorded vehicle vertical accelerations in excess of 2g. The system tested was designed to support a storage bin which could have a loaded weight greater than 30 lb. Most real-world usage centered about a zero mean load.

Four samples were tested with the stroke history. Samples 1 and 2 were repeated to check test variation. Each history consisted of a defined block of about 370 reversals incremented every 1.5 seconds. Samples were inspected for cracks at the conclusion of every other block. In addition, two samples were tested with a constant-displacement triangular waveform cycled at 0.5 Hz and checked for cracks every 5 minutes (150 cycles).

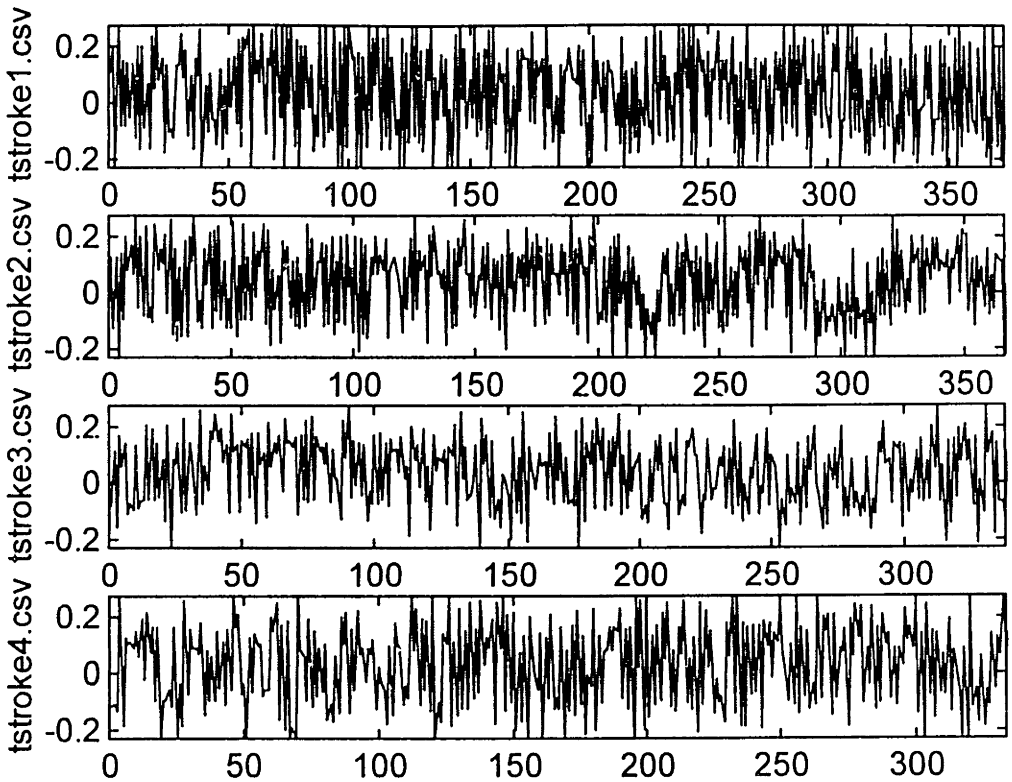

Figure 3-25: Tab Stroke Histories

Life calculations on the tab were made using the same method developed for road-load inputs on the test bars. A finite element analysis was run upon a model of the cut bin and rollover clip. It showed the greatest stresses appearing at the intersection of the tongue and the base of the three supporting gussets.

3.4.2 Result & Discussion

Since PFLAP accepts only load history input, each stroke history's observed load history was recorded from the test machine. Actual loads all were very close to the originally generated loads before the stroke conversion. The load history usually displayed a slight drop in applied loads in the first few passes of the stroke history, but remained otherwise stable. Figure 3-19 shows the actual recorded load under each repeated pass of stroke history "tstroke3" for selected reversals.

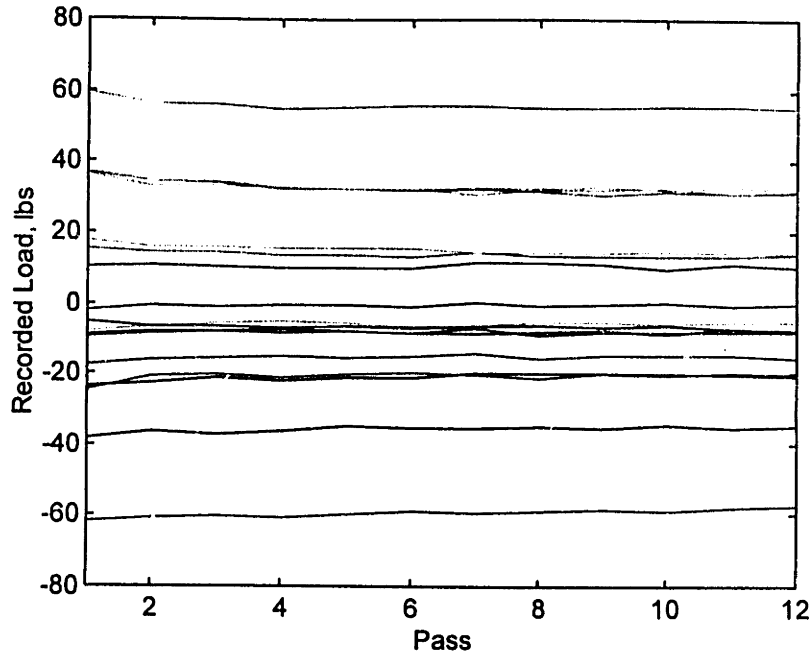

Figure 3-26: Load Recorded during Repeated Stroke History

Predictions were made based upon the entire load history from test start to initiation. This allowed PFLAP to consider any changes in load amplitudes which may have occurred from pass to pass during cycling. Figure 3-27 shows each profile's observed load history and an estimated strain histogram for the most stressed element. Note that this histogram was generated using the finite element solution for the given geometry and the Neuber's rule nonlinearity correction. The frequency scales on this graph are much larger than those seen on Figure 3-14 and Figure 3-15 since they are representative of several passes of the profile.

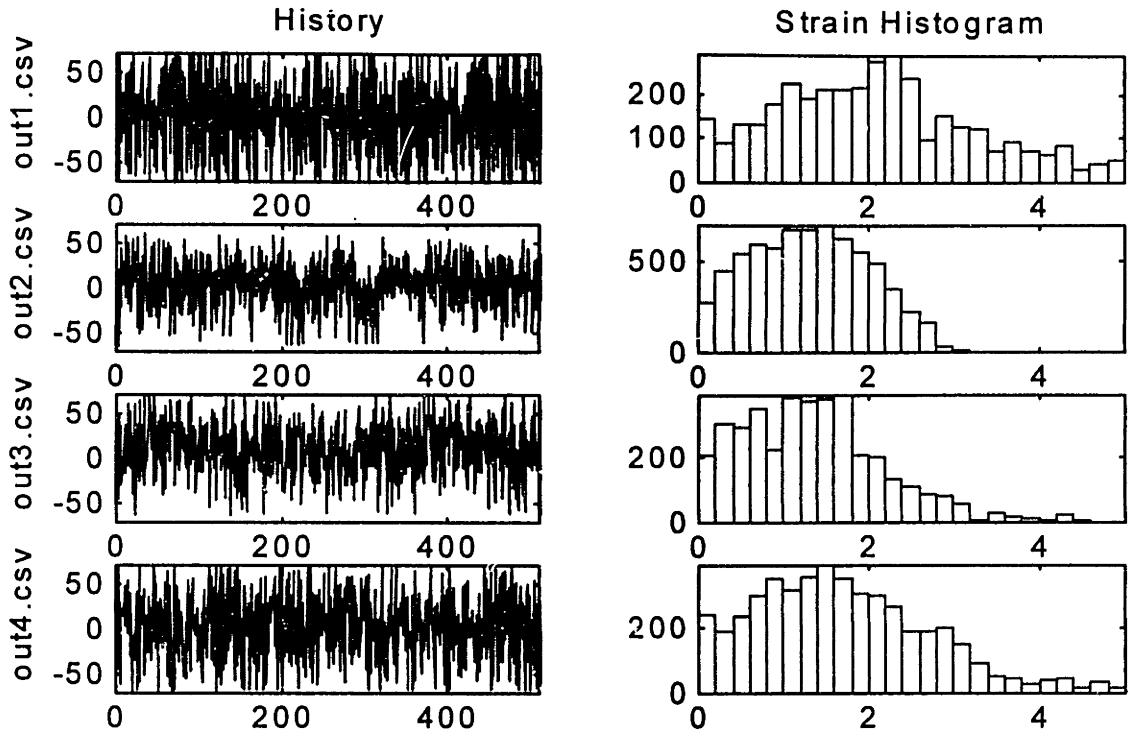

Figure 3-27: Recorded Load Histories - Tab Cycling

A complete run of the PFLAP program produced a life prediction for each element. These numbers were imported into the finite element mesh and displayed. The numbers in the legend are in the form of $\log(2N_i)$. The rollover clip is plotted transparently for easier visibility of the critical tab section.

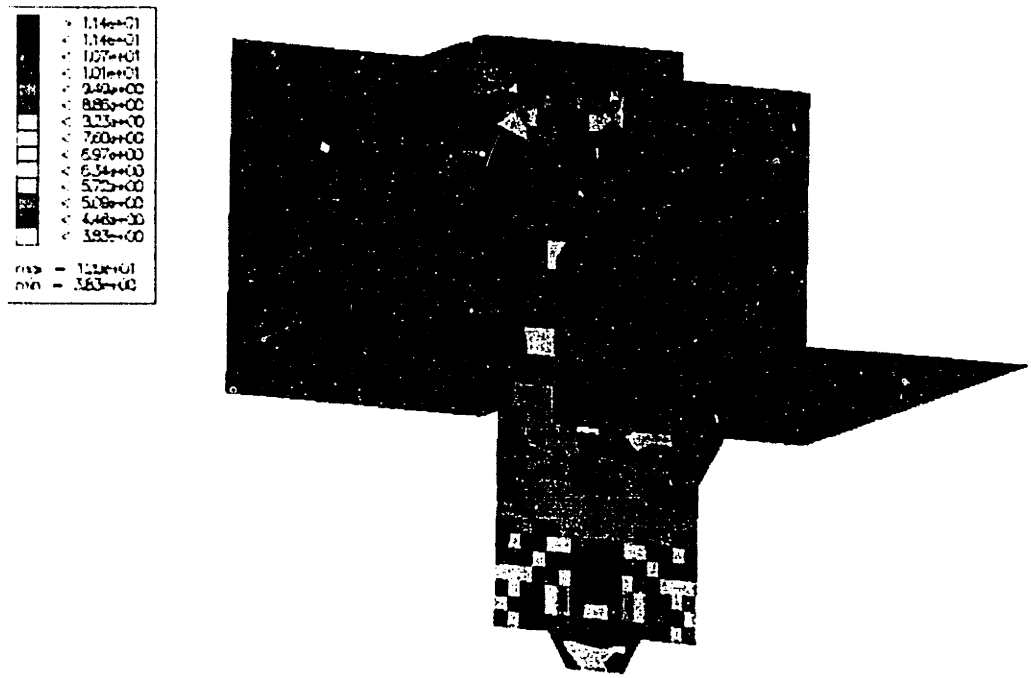

Figure 3-28: Sample PFLAP output

Each PFLAP prediction was plotted against the actual cycling result as in Figure 3-19. Figure 3-29 presents both the constant triangular waveform and the stroke history results.

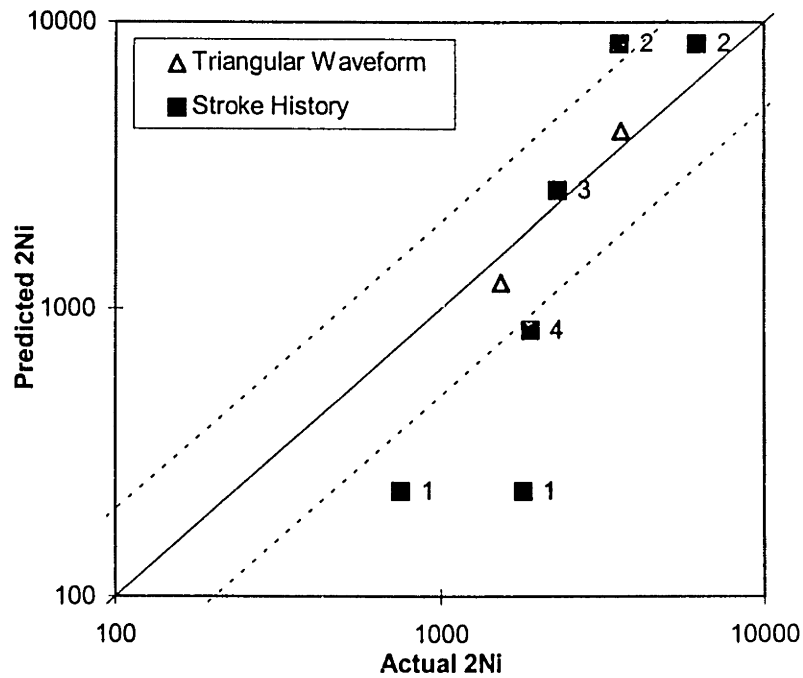

Figure 3-29: Tab Cycling Predictions

The average prediction error for the stroke history tests is 67%. This is greater than the error seen in the sample bar load history tests. The stroke history data show conservative results for short tests and nonconservative results for long-duration tests. The data trend is approximately linear, but does not have the same slope as the 1:1 line. A possible interpretation of this result is that predictions could have been more accurate given a different strain-life curve.

The repeatability of this test is low. Tests 1 and 2 were conducted twice and display final cycling lives differing by 82% and 53% respectively[4]. This difference in seemingly identical tests corresponds to the low repeatability observed in the sample bar load history tests and the strain-life curve generation.

All data points contain error relating to the part inspection interval. Since samples were only inspected during a certain time interval, cracks may have appeared before the inspection. As in the test bar case, though, inspection intervals were decreased as initiation was believed to be imminent.

There are three primary sources of error which will influence a fatigue life prediction.

1) Failure to accurately predict the strain amplitudes in the part. This results from errors in the finite element solution or in the application of Neuber's Rule.

2) Failure to reference the predicted strain amplitude to the proper constant-amplitude life. This scatter can be the result of sensitivity to small changes in test conditions or from actual material differences resulting from batch or processing variation.

3) Failure of the cumulative damage law to sum constant-amplitude lives to a multiple-strain reversals-to-initiation.

The strain-life curve generation conducted in section 3.1 contained only type 1 error since the stress state of the bar was well known and the bar was cycled at constant strain. The variable-strain bar tests conducted in section 3 contain type 1 and type 3 error. The stroke history tests in section 3.3 contain error types 1-3. If one assumes that the average error contributed by each error type to each test is the same, it is possible to estimate the contribution of

---

[4] These percentages calculated with respect to the average of the two lives.

each error type in isolation. With this assumption, the error contributed by strain-life scatter (type 1) is about 35%. The error contributed by damage accumulation (type 3) is about 40-35=5%. Lastly, the error due to improper evaluation of the strain history is 66-35-5=26%. From this analysis, we see that more than half of the error is contributed by the intrinsic difficulty of predicting polymer fatigue lives under near-ideal conditions. Figure 3-30 shows the relative contribution of each error type.

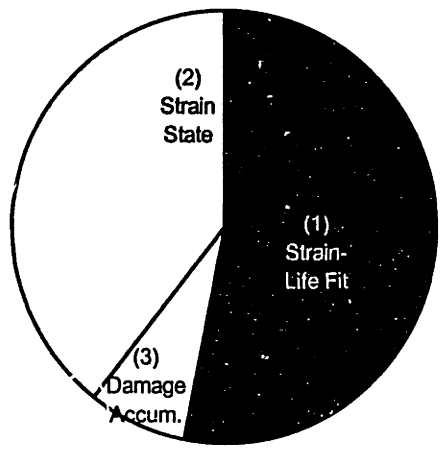

Figure 3-30: Relative Error Contributions

4. FURTHER STEPS

This thesis has investigated only one material and one part. In order to verify the method presented here, it is important to ensure that the process is robust and applies to a variety of materials, geometries, and loading conditions. A strain-life curve database should be constructed for commonly-used materials. This information could then be used in an analysis of components which are already being tested for durability, thus allowing a broad correlation study. Especially important to future applications is the use of PFLAP with a reinforced plastic. As polymers move into structural areas, they often include chopped glass to improve their strength. It is unknown whether the theory used in PFLAP will apply to random-orientation composite materials.

Weathering is an important issue in polymers. It has been shown that changes in molecular weight as the result of solar UV soaking can affect strain-life behavior. Exposure to hostile chemicals, such as oils and lubricating

greases, also affects the strain-life curve. Even exposure to water can alter material durability. (Yagasi and Kimura 1993) Environmental effects are important factors which merit further investigation. Unfortunately, it is even more difficult to predict the environmental exposure experienced by a part than it is to estimate service loads. Due to the wide range of exposure conditions and the very large amount of data required to generate strain-life curves for each condition, exposure effects were not covered in this paper. It may be worthwhile to generate a strain-life curve for a common material under a worst-case environmental exposure condition in order to evaluate the potential effects of weathering.

As was stated earlier, the purpose of this thesis was to investigate material properties since strain-life behavior forms the largest obstacle to the implementation of durability analysis routines for polymers. However, issues encountered during the finite element generation of a strain history (the second step of durability analysis) have pointed to areas which need further development. Generation of an accurate stress state may account for slightly less than half of all prediction error. Since the other half (data scatter) is mostly intrinsic to plastics and can only be solved with more intensive and expensive testing, the area of stain history calculation is the most promising one for further development.

1. PFLAP is based upon a static analysis. Since most in-vehicle random loading is a dynamic event, a dynamic finite element analysis is more appropriate for making predictions. Unfortunately, strain amplitudes are extremely sensitive to small changes in damping ratios when performing such a dynamic analysis. The damping behavior of polymers is difficult to predict, inserting a large unknown into the method. Work is needed in order to bring greater predictive capability into damping ratio selection. Note that all testing conducted in this investigation was static in application of loads.

2. A nonlinear analysis may prove useful in determining true stresses in the part. Neuber's rule is only an approximation of nonlinear response. An actual nonlinear analysis would be more computationally intensive, but may yield more meaningful results.

3. Prestresses which form during cooling can dramatically alter the stress state found in a plastic part. The strain-life curve is very shallow, causing small changes in stress to result in large changes in cycles-to-initiation. Since crack initiation is sensitive to small changes in stress, it is worth developing a method which will allow

the inclusion of prestresses in the finite element analysis. It may be worthwhile to perform a mold flow analysis upon the part to estimate the location and magnitude of prestresses in the part.

4. Material anisotropy may merit further investigation. Young's Modulus does not change significantly when testing longitudinal or transverse to the grain, which makes the finite element stress state reasonably accurate regardless of microstructure. However, the strain-life curve may be different depending on grain direction relative to the loading direction. All testing was conducted on bars cut with the grain longitudinal to the loading direction and none of the referenced sources mentioned grain direction as a test parameter. This variable deserves future study. If it is discovered that strain-life behavior is significantly different depending on load direction within the microstructure, it may be necessary to improve the current methodology by performing a mold flow analysis upon the part in order to determine grain direction at all locations in the part. Different material properties could then be assigned to each individual element based upon the predicted microstructure in that region.

A re-evaluation of the entire fatigue design philosophy may also be in order. Advanced computational tools may allow the calculation of fatigue lives given complex loading histories, fully characterized material data, and a set rules and relations which will produce a fatigue life prediction. Given the necessarily approximate nature of each step in the assumption chain, it seems that adding yet more detail to the analysis will only serve to increase effort and complexity with only marginal gains to prediction accuracy. The immense data requirements of these increasingly complex methods require that more effort be invested into testing abstract concepts.

A hybrid method might be developed which combines the fundamental mechanics of a full analytical fatigue calculation with the immediate applicability of the current component testing method. This would use only a small number of points on a strain-life curve to define some sort of desired life. When designing part geometry, the analyst could use a best guess of real-life loading conditions to insure that the part would never exceed this strain limit. Such a method would be conservative, but would insure that the part would live longer than some defined minimum duration. Design iteration during a full fatigue analysis essentially consists of raising or lowering part stresses by changing geometry. Simply setting a target stress removes several steps from the analysis and makes the relationship between geometry and fatigue life much more transparent. It is worth investigating whether this

simpler method would be so conservative that the extra part weight incurred through more cautious designs would counterbalance the time and savings gained through lower data requirements and fewer analysis steps.

5. CONCLUSION

This thesis presents an evolutionary step toward predictive iterative design for durability with plastics. This investigation has applied the logic of conventional fatigue methods to the problem of predicting mechanical fatigue life in polymers. It has shown that when properly modified, existing methods work roughly as well for EM3110 polycarbonate as they do for metals. The main contributor to prediction error is scatter in the strain-life curve, an intrinsic and unavoidable property of plastics. The other major contributor to error is prediction of the stress state in the component, which could be improved with further investigation. While the method presented here will not completely replace all physical testing, it can allow iterative design for durability at an early stage of the development process. This will allow polymer designers to optimize their structures without costly and time-consuming physical experimentation. By harnessing the power of polymer durability simulation, engineers can reduce cost and development time while improving the quality of their components.

6. REFERENCES

1. Agrawal, Conle, et al (1996) "Upfront Durability CAE Analysis for Automotive Sheet Metal Structures" SAE 961-053, presented at the International Congress & Exposition, Detroit, MI February 26-29, 1996
2. Beardmore & Rabinowitz (1975) "Fatigue Deformation of Polymers" *Treatise on Materials Science and Technology* **6**, 267-331
3. Beardmore (1978) "Fatigue Behavior of Polymers" in *Fatigue Mechanisms*, proceedings of an ASTM-NBS-NSF symposium, Kansas City MO May 1978. ASTM STP 675 pp. 453-470.
4. Buch (1975) "Verification of Various Methods for Fatigue Notch Effect Estimations in Case of Aircraft Metals" *Engineering Fracture Mechanics* **7**, 661-671
5. Conle (1977) "Verification of a Neuber-based Notch Analysis by the Companion-specimen Method" *Experimental Mechanics*, pp. 57-63
6. Conle, Oxland, Topper (1988) "Computer Based Prediction of Cyclic Deformation and Fatigue Behavior" *Low Cycle Fatigue, ASTM STP 942* American Society for Testing and Materials, Philadelphia pp. 1218-1236
7. Conway & Sjodahl (199`) "Analysis and Representation of Fatigue Data" Materials Park OH: ASM International
8. Crawford & Benham (1975) "Some Fatigue Characteristics of Thermoplastics" *Polymer* , **12** , 908
9. Devlukia (1987) "Experiment and Analytical Techniques for Assessing the Durability of Automotive Structures" SAE 871968, presented at the 1987 SAE Passenger Car Meeting and Exposition, Dearborn, MI October 20-21, 1987
10. Dowling (1993) "Mechanical Behavior of Materials" New Jersey: Prentice Hall
11. Fash (1987) "Enhancing the Design Development Cycle Through Computer Integrated Engineering for Durability" SAE 871942, presented at the 1987 SAE Passenger Car Meeting and Exposition, Dearborn, MI October 20-21, 1987
12. Glinka (1985) "Calculation of Inelastic Notch-Tip Strain-Stress Histories Under Cyclic Loading" Engineering Fracture Mechanics 22, 839-854
13. Hashin and Laird (1980) "Cumulative Damage Under Two Level Cycling: Some Theoretical Predictions and Test Data" *Fatigue of Engineering Materials and Structures*, **2** 345-350
14. Hay (1987) "Vehicle Load Histories: The Duality of Vibration and Fatigue Spectra" SAE 871938, presented at the 1987 SAE Passenger Car Meeting and Exposition, Dearborn, MI October 20-21, 1987
15. Hertzberg & Manson (1980) "Fatigue of Engineering Plastics" New York: Academic Press
16. Heyes (1995) "Assessment and Use of Linear Static FE Stress Analysis for Durability Calculations" SAE 951101
17. Iida, Takahasi, Ikai (1993) "A Regressive Expression of Fatigue Stress-Strain Behavior" Fatigue '93 Proceedings of the Fifth International Conference on Fatigue and Fatigue Thresholds Montreal, Quebec, Canada pp. 1631-1636
18. Kramer & Berger (1990) "Fundamental Processes of Craze Growth and Fracture" in *Advances in Polymer Science*, vol 91/92, p. 1-68. Berlin: Springer-Verlag
19. Kramer (1983) "Microscopic and Molecular Fundamentals of Crazing" in *Advances in Polymer Science*, vol 52/53 pp. 1-56. Berlin: Springer-Verlag.
20. Leis, Gowda, Topper (1973) "Some Studies of the Influence of Localized and Gross Plasticity on the Monotonic and Cyclic Concentration Factors" *Journal of Testing and Evaluation* **1**, 341-348
21. Lutes, Corazao, Hu, & Zimmerman (1984) "Stochastic Fatigue Damage Accumulation" Journal of Structural Engineering **11**, 2585-2601
22. Manson, Freche, and Ensign (1967) "Application of a Double-Linear Damage Rule to Cumulative Fatigue" ASTM STP 415 *Fatigue Crack Propagation*, 384

23. Miller and Zachariah (1977) "Cumulative Damage Laws for Fatigue Crack Initiation and Stage I Propagation" *Journal of Strain Analysis*, **12** 262-270
24. Mitchell (1987) "Evolution of Fatigue Design and Evaluation Technologies" SAE 871936, presented at the 1987 SAE Passenger Car Meeting and Exposition, Dearborn, MI October 20-21, 1987
25. Pompetzki, Topper, DuQuesnay, Yu (1990) "Effect of Compressive Underloads and Tensile Overloads on Fatigue Damage Accumulation in 2024-T351 Aluminum", Journal of Testing and Evaluation **1**, 53-61
26. Rice, Leis, & Nelson (1988) "Fatigue Design Handbook AE-10, Second Edition" Warrendale: Society of Automotive Engineers
27. Riddell, Koo, & O'Tooie (1967) "Fatigue Mechanisms in Thermoplastics" *Polymer Engineering and Science* **6**, 363-8
28. SAE J1099 (1977) "Technical Report on Fatigue Properties" Society of Automotive Engineers, Warrendale PA
29. SAE (1989) "Multiaxial Fatigue: Analysis and Experiments" Society of Automotive Engineers, Warrendalle PA
30. Sauer (1978) "Static and Dynamic Properties of Monodisperse Polystyrenes: Influence of Molecular Weight" *Polymer* **19**, 859-60
31. Sauer, Foden & Morrow (1977) "The Influence of Molecular Weight on Fatigue Behavior of Polyethylene and Polystyrene" *Polymer Engineering and Science* **17**, 246-50
32. Seeger & Heuler (1980) "Generalized Application of Neuber's Rule" *Journal of Testing and Evaluation* **8**, 199-204
33. Suresh (1991) "Fatigue of Materials" New York: Cambridge University Press
34. Tada, Paris, and Irwin (1985) "Stress Analysis of Cracks Handbook" St. Louis: Paris Productions Incorporated
35. Takemori and Morelli (1981) "Designing to Avoid Fatigue Failure in Engineering Polymers" SAE 811352, presented at the 1981 Automotive Plastic Durability Conference and Exposition, Troy, MI December 1-3, 1981
36. Thang et al (1971) "Cumulative Fatigue under Stress Controlled Conditions" *Transactions of the ASME, Journal of Basic Engineering*, 691
37. Thomas (1987) "Vehicle Modeling and Service Loads Analysis" SAE 871940, presented at the 1987 SAE Passenger Car Meeting and Exposition, Dearborn, MI October 20-21, 1987
38. Tipton (1991) "A Review of the Development and Use of Neuber's Rule for Fatigue Analysis" SAE 910165
39. Yagasaki and Kimura (1993) "The Effects of Water on the Fatigue Characteristics of Sheet Molding Compound and its Degradation Mechanisms" Fatigue '93 Proceedings of the Fifth International Conference on Fatigue and Fatigue Thresholds Montreal, Quebec, Canada pp. 1423-1428
40. GE Select (1995) Version 1.0b by GE Plastics
41. American Society of Metals (1986) "Atlas of Fatigue Curves" Metals Park, OH American Society of Metals
42. Skelton (1987) "High Temperature Fatigue: Properties and Prediction" New York Elsevier Applied Science